On the Development of a Parametric Aerodynamic Model of a Stratospheric Airship

Jesús Gonzalo*, Diego Domínguez, Adrián García-Gutiérrez, Alberto Escapa

Universidad de León, Aerospace Engineering Area, Campus de Vegazana s/n, León, 24071, Spain

Abstract

Following the current resurrection of large airship projects for stratospheric flight, a first-order potential flow panel method is presented to calculate pressure coefficients on a parametrically defined airship. Airships need three-dimensional grid definitions that often make difficult the execution of simple codes for preliminary results. A mesh-generation mechanism, appropriate for panel methods, is developed considering the different characteristic lengths of hull and fins. Thick and thin panels are defined, combined and properly attached among them to model the airship shape and the wake discontinuity surface. The classical formulation has been customised to both efficiently solve the potential problem and to derive interesting variables such as local velocity and surface pressure. After individual validations with thick ellipsoids and flat wings respectively, the solutions for the full vehicle

* Corresponding author; email: jesus.gonzalo@unileon.es

Please, cite as:
Gonzalo, J., Domínguez, D., García-Gutiérrez, A., & Escapa, A. (2020).
On the development of a parametric aerodynamic model of a stratospheric airship. Aerospace Science and Technology, 107, 106316.

are compared to tunnel tests of a representative airship body (Gertler 4154 Series 58) with fins. Pressure coefficient distribution and pitch moment coefficients of the body are predicted with very high accuracy. Even using only less than 4000 panels, overall error is smaller than about 5% and essentially null for the first half of the body. Furthermore, the speed of the problem setup and the solver make the development very appropriate to analyse preliminary designs under different flight conditions.

Keywords: high altitude platforms; airships; pseudo-satellite; HAPS; panel method, aerodynamics; stratospheric flight

1. Background and introduction

Recently airships have once again gained popularity as a form of pseudo satellites which can operate in the stratosphere [1]. Despite the low air density at these altitudes, winds are moderate. The combination of light materials and efficient energy management enable long endurance missions and this is encouraging many private and public organisations to develop precursor prototypes.

Aerodynamic performance of these vehicles is a key design feature. They usually implement a station-keeping control strategy where optimized propulsion plants [2] are needed to overcome aerodynamic drag. However, drag is not the only important characteristic. Aerodynamic lift, lateral forces and pitch and yaw momenta are major driving actions together with propulsion. In particular, the inherently instable pitch and yaw moment around the centre of thick bodies like airships may lead to control difficulties to the pilot [3], [4]. Thus, the aerodynamic analysis of the different design choices that should be made for the body shape

Please, cite as:
Gonzalo, J., Domínguez, D., García-Gutiérrez, A., & Escapa, A. (2020).
On the development of a parametric aerodynamic model of a stratospheric airship. Aerospace Science and Technology, 107, 106316.

and tail fins is critical in order to ensure an appropriate stability and controllability of the platform []. An excess in stability and controllability may have undesired impact on drag.

Numerical methods for aerodynamics prediction have been developed from the very beginning of the history of digital computation. In particular, the solution for inviscid potential flow around thin aerofoils was successfully addressed analytically by perturbation models, and then extended numerically to thick objects, even in 3D, by the so-called panel method [6]. Lighter than air vehicles were also studied with these methods, in an attempt to capture blunt body effect on lift by locating thin panels within the body [7]. Those theories became popular in the 1980s with the development of many commercial codes [8], until they were finally overcome by finite volume (fuzzily addressed as computer fluid dynamic —CFD—) methods.

Although nowadays the computer throughput is much more affordable, there are still limitations in the usage of powerful CFD codes. First, many of those are expensive. Second, they require the meshing of the whole fluid domain, which is tricky for even simple geometries. Finally, the configuration of the solver is complex, due to the presence of many options in the discretisation schematics, equation simplifications and data postprocessing. Assuming all these hurdles are passed, the computer load required is huge even for preliminary results. But the prize is very valuable as these methods have proven to be accurate in spite of having difficult aerodynamic conditions such as thick boundary layers, wake detachments, heat transfer or shock waves [9].

Aircrafts are large and fly at moderate speed, so Reynolds numbers are large [1] although in stratospheric conditions. This justifies the hypothesis of potential flow around the body. Moreover, attack and sideslip angles need to be small if a minimum of aerodynamic efficiency is sought, so the boundary layer is attached. When this does not occur, the detachment is

Please, cite as:
Gonzalo, J., Domínguez, D., García-Gutiérrez, A., & Escapa, A. (2020).
On the development of a parametric aerodynamic model of a stratospheric airship. Aerospace Science and Technology, 107, 106316.

confined to a small area around the rear part of the hull; ideally, the fins are large enough to not be seriously affected.

Under these conditions, many authors have applied the panel method for the optimum definition of airship shape [10], [11]. Besides, dynamics given by control surfaces can also be solved [12], even in stratospheric conditions [13] with the aid of these techniques. Some of those studies use analytic validation methods for revolution bodies, and many others involve wind tunnel tests. In most cases they are focused on specific designs and non-generic shapes or configurations. In airship on-design multidisciplinary optimisation, surrogate models for the aerodynamic performance are often proposed to avoid online CFD calculations since they are heavy [14].

In general, viscous effects are added to the potential flow results to model both laminar and turbulent contributions [15]. That can be done coupling the integral boundary-layer equations with the panel method [16]. Imaginative add-ons have been developed to provide classic panel methods with the ability to model detached flows and propulsion wake effects [17], although very few details about the used particular implementation were provided. There are also extensions to cope with unsteady flow, allowing for the estimation of added masses [18], [19].

The objective of this paper is to progress on the work of the previously mentioned authors by developing a customised first order panel method to solve the potential flow problem around an airship whose geometry is parametrically defined, paving the way for the execution of optimisation codes even during preliminary design phases. The grid generation method and the panel solver must be integrated together to seamlessly produce accurate results for all feasible input parameters considering attached flows and low angles of attack/sideslip. The

Please, cite as:
Gonzalo, J., Domínguez, D., García-Gutiérrez, A., & Escapa, A. (2020).
On the development of a parametric aerodynamic model of a stratospheric airship. Aerospace Science and Technology, 107, 106316.

classical formulation needs to be customised to both efficiently solve the potential problem and to derive interesting variables such as local velocity and surface pressure. Besides, the accuracy of the method is to be checked against experimental tests with the available hull shape. The final goal is to enable the utilisation of the proposed method as the foundation of many other studies based on aerodynamic performance of airships, avoiding the need for case-by-case mesh definition and solver configuration. The method is specifically applicable to large stratospheric airships, where missions are designed to keep optimum aerodynamic configuration most of the time, with slow manoeuvres at low angles of attack and, hence, attached flow. In most current designs, these huge bodies are equipped with stabilisation fins to fly for weeks in slow station-keeping missions.

The panel method is ideally suited to the goals of this paper, as it provides a mechanism to make a preliminary estimation of aerodynamic performance in a much simpler manner with respect to CFD codes. In the panel method there is no need to define a grid throughout the flow field but only a 2D mesh on the boundary of the flying object and its wake. This makes it possible to perform parametric sensitivity analysis and optimisation processes that could not be feasible with more complex models. Considering the execution time required to produce a result for a given airship with fins at a single flight condition, a quite simple CFD simulation would require a mesh with at least a few millions of cells and it would take several hours to be finished even if multiple processors are used. However, the equivalent panel method just needs about four thousand cells and it is solved in a matter of seconds.

Airship models are a mix of thick and thin elements. Current codes are not always prepared to deal with these types of attachments because in many cases only one type of panel is available. Other commercial examples such as VSAERO [20] or NEWPAN [21] does not

Please, cite as:
Gonzalo, J., Domínguez, D., García-Gutiérrez, A., & Escapa, A. (2020).
On the development of a parametric aerodynamic model of a stratospheric airship. Aerospace Science and Technology, 107, 106316.

clearly explain how interpolation is developed to deal with the thick-thin panel interaction. On its side, classical PANAIR [22] is powerful but difficult to configure for the optimisation of airship shapes. Other codes are focus on the design of typical transonic transport aircraft configurations as, for example, VGK, BVGK [23] and VFP [24]. More modern options such as APAME [25] or OpenVOGEL [26] are promising but still do not consider thin panels. In general, the efforts carried out in [7] to apply potential methods to airships, more than three decades ago, did not lead to the spectacular evolution of those ones dedicated to aerofoils (such as popular XFOIL, XFLR5 or FLOW5). More recent investigations go into great detail regarding particular airship shapes, like Akron [27] or LOTTE [17], [28] models, moving the latter quickly from potential methods to more sophisticated CFD analysis and experimental testing.

As a consequence, a panel method specifically dedicated to airships is not currently available. This method, when properly validated, may fill the gap between powerful but complex generic codes (panels or CFD) and basic hull-fin interaction estimates [29] that are available from decades. The specific needs driving the research are:

- Automated and straightforward definition of the hull and fins from few geometric parameters
- Automated meshing of vehicle and wakes
- Automated panel design, with seamless thin-thick and thin-wake panel interactions and proper neighbour relationships
- Potential problem definition from a mix of Neumann and Dirichlet boundary conditions
- Quick solver and post-processor to evaluate velocities and pressures and hence aerodynamic forces and torques

Please, cite as:
Gonzalo, J., Domínguez, D., García-Gutiérrez, A., & Escapa, A. (2020).
On the development of a parametric aerodynamic model of a stratospheric airship. Aerospace Science and Technology, 107, 106316.

Airship design processes shall take advantage of this quick code as part of automatic optimisation algorithms. Besides, the research can serve as a baseline for future additions that overcome panel method limitations.

- The paper is organised in the following way. First it is presented the development of the method, including the modelling of thick and thin surfaces, wakes and general equations to solve the problem. The details provided make possible to fully reconstruct the code to any interested reader. This presents an important difference with previous works in the field, where usually only a general description of the method and its implementation is provided. After that, section 3 includes the validation of the code using well known analytic results for thin and thick objects. Once the capability to produce accurate results for simple geometries has been proved, section 4 fully analyses the ability of the method to model realistic airship configurations, comparing the predictions with real experimental data obtained in wind tunnel tests. Finally, some conclusions are drawn where the validity of the proposed methodology is stated. For the sake of clarity, the basic principles and equations of panel method formulation have been included in Annex.

2. Development of the airship panel method

In the panel method, the potential flow Laplace equation solution is formed by a sum of source and doublet distributions on the boundary, including the object and the wake [30]. Generally speaking, sources are appropriate to implement the thickness of the object whereas doublets (or vortex) involve antisymmetric flow typically in thin surfaces and wakes. Neumann (body impenetrability) and Dirichlet (constant potential function inside the body) boundary conditions must be applied. Additionally, the circulation around the body is

Please, cite as:
Gonzalo, J., Domínguez, D., García-Gutiérrez, A., & Escapa, A. (2020).
On the development of a parametric aerodynamic model of a stratospheric airship. Aerospace Science and Technology, 107, 106316.

essentially linked to the shape and location of the wakes, which is equivalent to the two-dimensional Kutta condition.

In this study, a first-order method is proposed where the geometry is modelled by small flat panels with constant distribution of sources and doublets. In this case, only quadrilateral and triangular panels are considered. If a four-sided panel is not flat, it is divided into two triangles or an approximate quadrilateral panel with the same surface and an average normal.

For the steady irrotational flow, the formulation in terms of potential function ($\emptyset$) instead of body-fixed velocity (u, v, w) is preferred. The relation of both is $\nabla\emptyset = \bar{V}$. The use of the single scalar field as unknown saves memory and speeds up the whole process. Hence, incompressible flow continuity becomes the main equation to solve, i.e. the Laplace equation:

$$\nabla^2\emptyset = 0. \tag{1}$$

Following the first Green's identity [30], a general solution in the form:

$$\emptyset = -\frac{1}{4\pi}\int_{body}\left[\sigma\left(\frac{1}{r}\right) - \mu\bar{n}^* \cdot \nabla\left(\frac{1}{r}\right)\right] dS + \emptyset_\infty, \tag{2}$$

where r is the modulus of the position vector, $\bar{n}^*$ is the body surface normal unit vector towards the interior, S denotes the body surface, σ the strength of the source kernels and μ the same for the doublet ones. The scalar field $\emptyset_\infty$ is the potential corresponding to unperturbed freestream; for cruise conditions at velocity $\bar{V}_\infty = (U_\infty, V_\infty, W_\infty)$ in Cartesian coordinates, it can be written as:

$$\emptyset_\infty = U_\infty x + V_\infty y + W_\infty z. \tag{3}$$

Furthermore, should sources be allocated to thick panels only, the expression for the potential in the flow surrounding the object becomes:

Please, cite as:
Gonzalo, J., Domínguez, D., García-Gutiérrez, A., & Escapa, A. (2020).
On the development of a parametric aerodynamic model of a stratospheric airship. Aerospace Science and Technology, 107, 106316.

$$\emptyset = -\frac{1}{4\pi}\int_{body}\sigma\left(\frac{1}{r}\right)dS - \frac{1}{4\pi}\int_{body+fins+wake}\mu\bar{n}\cdot\nabla\left(\frac{1}{r}\right)dS + U_\infty x + V_\infty y + W_\infty z, \quad (4)$$

with a constant value for the potential internal to the body (e.g. zero or $\emptyset_\infty$). The lector should be aware of the direction of the normal phasor $\bar{n}$, taken to the outside of the body, as preferred in many meshing algorithms:

The Neumann boundary condition would be:

$$\left.\frac{\partial\emptyset}{\partial n}\right|_{boundary} = 0, \quad (5)$$

denoting n the normal direction of the boundary. If this occurs in the surface of a body without internal singularities, the internal potential needs to be constant, which is the Dirichlet equivalent boundary condition. However, other choices for $\emptyset_i$ are possible (even if not constant) to ease the equation forms, always respecting eq. (5) at the boundary. One of the most popular is selecting:

$$\emptyset_i = \emptyset_\infty = U_\infty x + V_\infty y + W_\infty z, \quad (6)$$

which is equivalent to think of $\emptyset$ as a perturbation potential (since internal potential removes the effect of freestream).

The solution (sources and double distribution) of eq. (4) is not uniquely defined. In order to reach that condition, a source distribution can be arbitrarily selected (doublet strength will change accordingly) and the Kutta condition must be forced.

With respect to the source distribution selection, aiming at reducing the strength of the doublets and minimising truncation errors in numerical algorithms, a constant internal potential is recommended based on the far field velocity [31]:

$$\sigma = -\bar{V}_\infty\cdot\bar{n} - V_{perm}, \quad (7)$$

Please, cite as:
Gonzalo, J., Domínguez, D., García-Gutiérrez, A., & Escapa, A. (2020).
On the development of a parametric aerodynamic model of a stratospheric airship. Aerospace Science and Technology, 107, 106316.

where V_{perm} accounts for possible wall permeability or blowers, positive towards $\bar{n}$. This last feature will not be used in this paper. The wake configuration and the Kutta condition are discussed later in this paragraph.

Now the potential flow problem has been reduced to finding the strength of a constant distributed sources and doublets in a number of flat panels throughout the surface of the body (N_B) and its wake (N_W). Moreover, eq. (7) fixes the values of sources, so Dirichlet condition in eq. (6) applied to eq. (4) leads to:

$$\sum_1^{N_B} \frac{1}{4\pi} \int_{panel} \sigma \left(\frac{1}{r}\right) dS + \sum_1^{N_B} \frac{1}{4\pi} \int_{panel} \mu \bar{n} \cdot \nabla \left(\frac{1}{r}\right) dS + \sum_1^{N_W} \frac{1}{4\pi} \int_{panel} \mu \bar{n} \cdot \nabla \left(\frac{1}{r}\right) dS = 0. \quad (8)$$

Naming $\emptyset_S$ the potential induced by a unit-strength source panel at certain position in the domain, and $\emptyset_D$ the equivalent by a unit-strength doublet, eq. (8) can be written:

$$\sum_1^{N_B} \sigma \emptyset_S + \sum_1^{N_B} \mu \emptyset_D + \sum_1^{N_W} \mu \emptyset_D = 0. \quad (9)$$

Now, if the geometry is to be given by a multitude of small flat panels, integrals in eq. (4) shall be split into a large sum of finite elements, each referred to one panel containing a constant distribution of doublets, sources or both.

2.1. Thick panels

A conventional panel with a distribution of kernels that includes sources is referred to as a thick panel. The panel represents the discontinuity in across-panel local velocity; intuitively, this is equivalent to splitting the incoming flow into two diverging directions as a 2D non-zero thickness object would do in normal flight.

Detailed formulation of first order panel geometry and kernel distribution used in this paper can be found in Annex: Basics of panel method.

Please, cite as:
Gonzalo, J., Domínguez, D., García-Gutiérrez, A., & Escapa, A. (2020).
On the development of a parametric aerodynamic model of a stratospheric airship. Aerospace Science and Technology, 107, 106316.

2.2. Thin panels

Thin panels are the limit of those conventional thick panels where the upper and lower sides are so close that the co-location point of both tend to be the same, as well as the boundary segments. In this situation, the resulting thin panel captures the combination of singularities of both sides. Should this fact be neglected, the influence coefficient matrix would have two identical lines, and then it would become singular.

Besides, this combination must consider the opposite directions of the normal of both original sides. If constant strength doublets are considered, the thin panel ends up with a new constant doublet with an intensity which is the subtraction of both. The normal of the thin panel is towards the upper side so it will be the upper doublet minus the lower doublet.

The sources, however, vanish. This is compatible with the mass conservation in the across-panel direction. The absence of internal potential in thin panels makes it interesting to apply Neumann's boundary conditions in those cases, eq. (5).

2.3. Wake panelling

The circulation in trailing edges can be shed along a wake. Wakes can be modelled by thin flat panels with uniform distributions of doublets, which is equivalent to a vortex ring. The wake modelled in this way equals to a number of vortex threads from the trailing edge to the infinite downstream (Figure 1). Since the effect of doublets/vortex vanishes with distance, the wake model can be stopped once a reasonable distance from the body has been reached.

Please, cite as:
Gonzalo, J., Domínguez, D., García-Gutiérrez, A., & Escapa, A. (2020).
On the development of a parametric aerodynamic model of a stratospheric airship. Aerospace Science and Technology, 107, 106316.

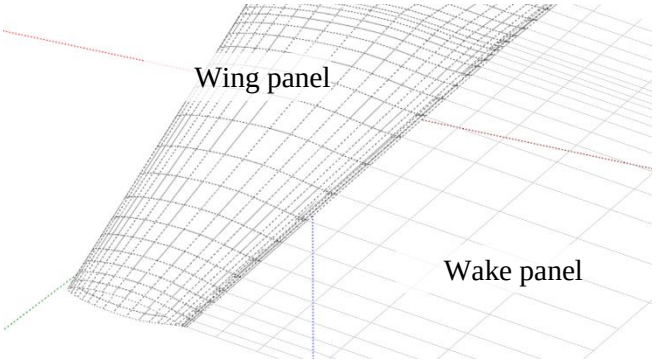

Figure 1: Wake panel model.

Each wake panel, by construction, should have lateral segments parallel to local velocity. Vortex lines not parallel to the local velocity vector would involve lift forces, which is not the case in a wake. This justifies the fact that every panel in the wake inherits the vorticity (or doublet intensity) of the upstream neighbour panel, so that the vortex of the shared front/rear segment is always null. The lateral segments of the panels form the above-mentioned streamline vortex threads.

The first panel in the wake takes its strength (μ_W) from the vorticity difference between upper and lower surfaces at the trailing edge (Figure 2). This is a three-dimensional implementation of the Kutta condition as the vortex intensity in the trailing edge becomes automatically null. The implementation is quite simple provided that the wake panels are directly linked, one on one, to couples of upper and lower surface panels forming a trailing edge.

$$\mu_W = \mu_{te\_u} - \mu_{re\_l}. \tag{10}$$

This implies that adding a wake does not increment the number of unknowns, as the wake panel doublet strength can be directly linked to the ones of the shedding panels. When zero thickness surfaces are modelled by a single panel sheet, the wake is fed by the circulation of the trailing edge [32]. Thus, condition of eq. (10) degenerates into:

Please, cite as:
Gonzalo, J., Domínguez, D., García-Gutiérrez, A., & Escapa, A. (2020).
On the development of a parametric aerodynamic model of a stratospheric airship. Aerospace Science and Technology, 107, 106316.

$$\mu_W = \mu_{te}. \tag{11}$$

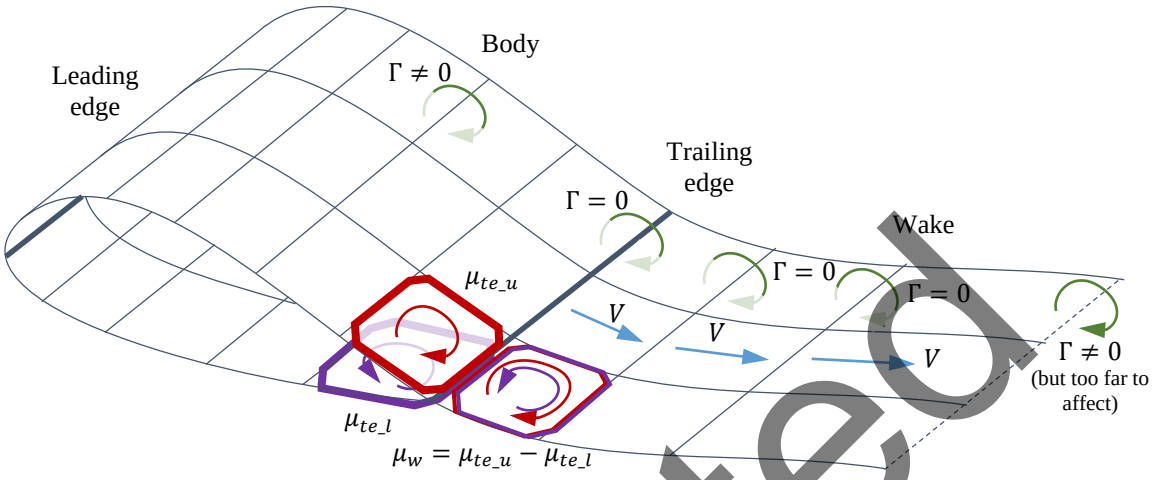

Figure 2: Scheme of vortex shedding.

Finally, in the case of non-lifting bodies with attached flow, the trailing point automatically meets the condition of no circulation shedding (Figure 3), if the / a triangle panel is used to close the rear part of the form. The vortex rings of those panels sum null regardless of the values which they have.

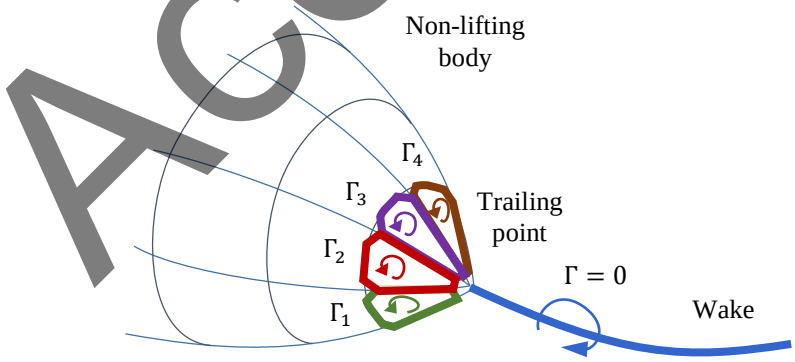

Figure 3: Trailing point of a non-lifting body.

The wake is not a physical membrane but an idealisation of a surface of discontinuity. That means that each doublet distribution, as seen as a four-segment vortex ring, must meet a zero-force condition. Attending to Kutta theorem, as has been mentioned above, each segment

Please, cite as:
Gonzalo, J., Domínguez, D., García-Gutiérrez, A., & Escapa, A. (2020).
On the development of a parametric aerodynamic model of a stratospheric airship. Aerospace Science and Technology, 107, 106316.

must be parallel to the local velocity. By construction, head and tail segments within the wake compensate with their front and back neighbours, so only lateral sides must be built to follow local velocity. As the wake deflection affects panel influence parameters, the process needs to be repeated iteratively. Figure 4 depicts wake deflections after several solve-move iterations. Typically, the loop converges after a few iterations, with stable pressure coefficients. In conventional wings, the deflection of the wake does not have a relevant effect on the final solution. In the case of complex configurations like in Figure 5 that statement is not so evident [30].

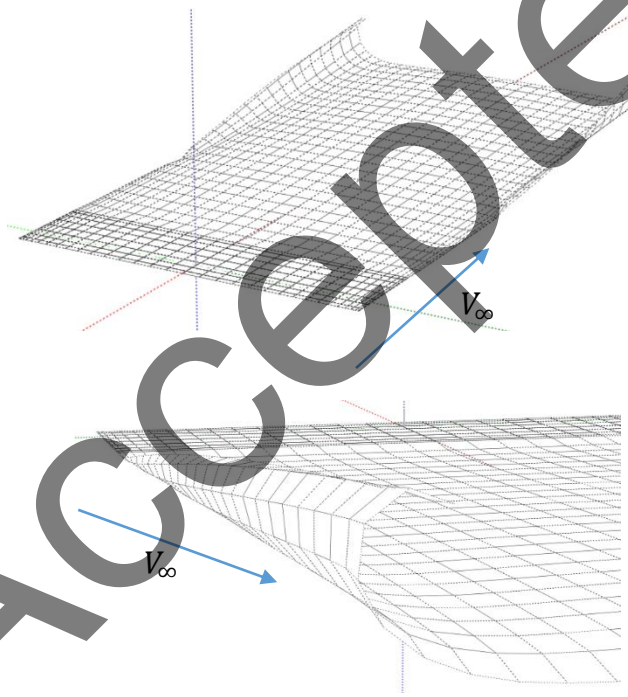

Figure 4: Example of vortex wake deflection after a flat rectangular wing.

Please, cite as:
Gonzalo, J., Domínguez, D., García-Gutiérrez, A., & Escapa, A. (2020).
On the development of a parametric aerodynamic model of a stratospheric airship. Aerospace Science and Technology, 107, 106316.

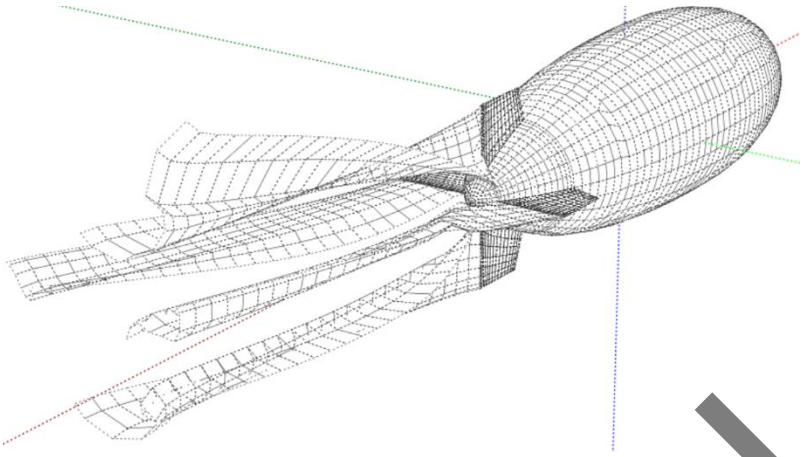

Figure 5: Example of wake deformation in a 4-fin airship with angles of attack and sideslip.

2.4. Algebraic equations

The resolution of eq. (9) is now addressed. The geometry has been reduced to flat panels, so $\emptyset_S$ is given by eq. (32) and $\emptyset_D$ by eq. (38). The source strength is set in eq. (7) and the wake vorticity is linked to the trailing edge panel vorticity in eq. (41). Thus, the only unknown is the double distribution on body surface μ, with a single value per panel. The equation, in matrix notation, can be written as:

$$[A][\mu] = [RHS], \tag{12}$$

where $[A]$ is the influence coefficient matrix and $[RHS]$ is the right-hand side vector.

Each row of $[A]$ corresponds to an 'effect' panel. More specifically, the effect received in the co-location point of a panel by the rest. Each column reflects the panel contributing to the total potential, that is to say the 'cause' panel. The diagonal is the potential effect of a doublet panel on itself, as stated in eq. (39); recalling that eq. (12) refers to the interior potential, the negative sign must be selected. Additionally, the trailing edge panels need to include the associated wake cause panels.

Please, cite as:
Gonzalo, J., Domínguez, D., García-Gutiérrez, A., & Escapa, A. (2020).
On the development of a parametric aerodynamic model of a stratospheric airship. Aerospace Science and Technology, 107, 106316.

We will notate with subscript i the effect panel (or its co-location centre) and subscript j the cause panel. Thus, $\emptyset_{S_{ij}}$ and $\emptyset_{D_{ij}}$ denote the potential induced by unitary sources and doublets of panel j in the centroid of panel i. Both i and j run from 1 to the number of panels on the body N_B. The wake panels are also cause doublets, but their intensities are a function of upper and lower sides of trailing edges. Thus, the influence parameter can be written as:

$$\begin{aligned} A_{ij} &= \emptyset_{D_{ij}} + \textstyle\sum_{wake} \emptyset_{D_{iw}}, && \text{when } j \text{ is a thick panel in the upper side of trailing edge,} \\ A_{ij} &= \emptyset_{D_{ij}} + \textstyle\sum_{wake} \emptyset_{D_{iw}}, && \text{when } j \text{ is a thin panel of trailing edge,} \\ A_{ij} &= \emptyset_{D_{ij}} - \textstyle\sum_{wake} \emptyset_{D_{iw}}, && \text{when } j \text{ is a thick panel in the lower side of trailing edge,} \\ A_{ij} &= \emptyset_{D_{ij}}, && \text{for rest of } j \text{ panels.} \end{aligned} \tag{13}$$

The RHS matrix is the result of the effects of source panels. If σ_i is the source strength in panel i as given by (7), the vector coefficients using Einstein notation are:

$$RHS_i = -\emptyset_{S_{ij}}\sigma_j. \tag{14}$$

2.5. Velocities and pressures

As a result of the third Green's identity, the perturbation potential in a panel equals its doublet strength [33]. The corresponding perturbation velocity can be obtained by derivation. The normal component is directly provided by the panel source intensity, as stated by condition of eq. (7). This provides a quick method for the calculation of perturbation velocity and eventually the pressure on the panel:

$$v_\xi = -\frac{\partial \mu}{\partial \xi} \qquad v_\eta = -\frac{\partial \mu}{\partial \eta} \qquad v_k = \sigma. \tag{15}$$

The total velocity in body and panel coordinates is given by:

Please, cite as:
Gonzalo, J., Domínguez, D., García-Gutiérrez, A., & Escapa, A. (2020).
On the development of a parametric aerodynamic model of a stratospheric airship. Aerospace Science and Technology, 107, 106316.

$$\bar{V}^P = L_{PB}\bar{V}_\infty + \begin{bmatrix} v_\xi \\ v_\eta \\ v_k \end{bmatrix}, \qquad \bar{V}^B = \bar{V}_\infty + L_{BP}\begin{bmatrix} v_\xi \\ v_\eta \\ v_k \end{bmatrix}, \tag{16}$$

where obviously $\bar{V}_z^P = \bar{0}$ in impermeable surfaces because the source was selected to be opposite to the free stream normal component and Neumann condition forces it.

And finally, with the module of the velocity vector in either frame and using the Bernoulli equation for steady incompressible flow, the pressure coefficient (c_P) is:

$$c_P = 1 - \left(\frac{|\bar{V}|}{V_\infty}\right)^2. \tag{17}$$

With respect to the estimation of the velocity and pressure in thin panels, the approach is slightly different. Induced perturbation velocity is very useful to calculate panel normal component, which, by the way, has already been forced to compensate that of the free stream.

For the tangential components, the well-known equivalence between a rectilinear sided panel with a constant doublet distribution and a vortex ring is used [30]. The circulation of the vortex is numerically the same as the doublet strength. As the panels are within a grid, the vortex intensity in each segment of the panel (γ_i) is the subtraction of the doublet strengths (μ) of the neighbour panels:

$$\gamma_i = \mu - \mu_{neighbour\ i}. \tag{18}$$

Attention must be paid to the units. Whereas the doublet intensity is a surface distribution, the vortex is a linear one.

Once the transformation between doublets and vortex is developed, the force on the panel can be estimated using the Kutta-Joukowski theorem. The induced tangential velocity in the panel, the perturbation one, can be expressed as:

Please, cite as:
Gonzalo, J., Domínguez, D., García-Gutiérrez, A., & Escapa, A. (2020).
On the development of a parametric aerodynamic model of a stratospheric airship. Aerospace Science and Technology, 107, 106316.

$$\bar{v}_t = \frac{1}{2S}\sum_1^4 \gamma_i \bar{n} \wedge \bar{d}_i, \tag{19}$$

where side vectors $\bar{d}_i$ are given in eq. (26), S is the surface of the panel and $\bar{n}$ the panel normal phasor. The vector product is used to isolate the tangential velocity from the total perturbation.

The full tangential velocity must represent the idealisation of a thin panel, where there is a sudden discontinuity in the perturbation tangential velocity ($\Delta\bar{v}_t$) in the two sides of the panel. In fact, the discontinuity is caused by the doublet in the own panel. Thus, it can be written:

$$\bar{V}_{t\_upper} = \bar{V}_\infty + \frac{1}{2}\Delta\bar{v}_t, \qquad \bar{V}_{t\_lower} = \bar{V}_\infty - \frac{1}{2}\Delta\bar{v}_t. \tag{20}$$

The Bernoulli equation provides information on the panel pressure difference (Δc_p) between its two sides:

$$\Delta c_p = c_{p\_upper} - c_{p_{lower}} = -2\frac{\bar{V}_\infty \bar{v}_t}{V_\infty^2}. \tag{21}$$

2.6. Airship parametrization. Mesh and panels generation

An airship is typically composed of a large hull, a relatively small car which includes the propulsion plant and tail control surfaces. From the aerodynamic point of view, the hull and the tail are the most interesting and attract the attention of designers.

The hull is considered a revolution body and, hence, defined by its length and its generatrix. In order to parametrise the geometry of the body, panels should be concentrated in the areas of steep changes of the flow variables as pressure and velocity. This occurs around the leading edge, the trailing edge and in the fin attachments. Thus, as developed in 2D codes for aerofoils, the along-axis panel size is taken from a cosine-based law from a total number of divisions. This law fosters the granularity at bow and stern. The fins only impose a restriction

Please, cite as:
Gonzalo, J., Domínguez, D., García-Gutiérrez, A., & Escapa, A. (2020).
On the development of a parametric aerodynamic model of a stratospheric airship. Aerospace Science and Technology, 107, 106316.

to that law: the leading edge and trailing edge at the attachment must coincide with the body panel vertexes. This is easily implemented by conditionals in the implementation of the along-axis body splitting.

The circumferential size is selected from a master number of across panels at body centre (normally close to the region where the hull is widest). This number is modulated with the local radius at each x-axis position so that the azimuthal size is approximately constant. The change in the number of panels of consecutive belts is accommodated using triangular panels (as shown in Figure 6 for different generatrix lines and later in Figure 9 for ellipsoids).

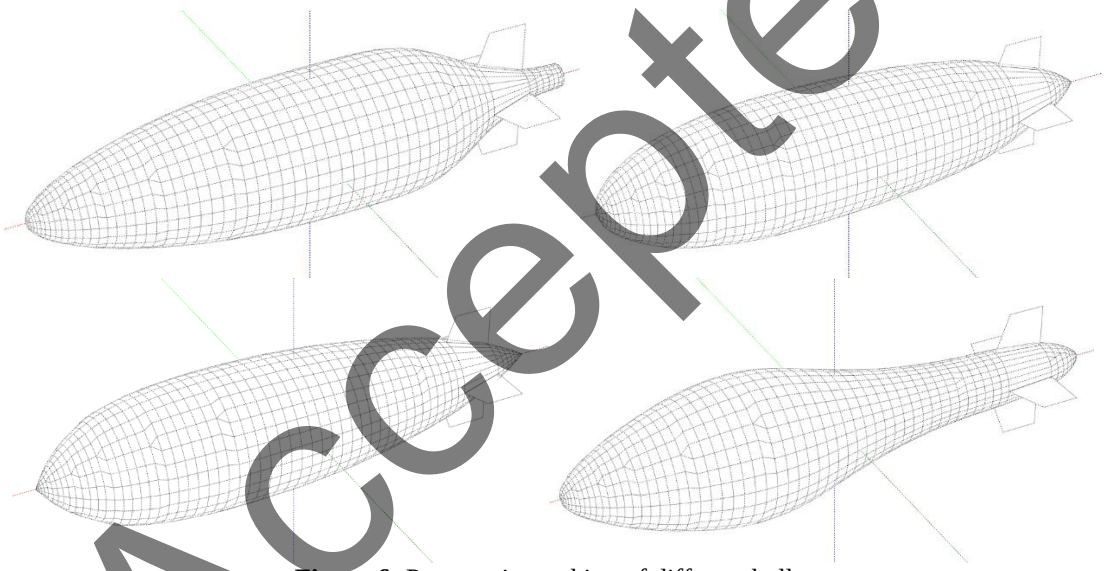

Figure 6: Parametric meshing of different hulls.

Fins are thin aerodynamic surfaces in the tail of the airship. They reduce the intrinsic instability of the hull and, if provided with moveable parts, enable the yaw and pitch control of the vehicle. Unfortunately, thin fins produce about one third of the vehicle total drag [4].

In this present study, two horizontal and two vertical fins are considered. From the perspective of the method, there is no intrinsic difficulties in managing other configurations, although this is the most popular since control in both axes is decoupled. In the particular case

Please, cite as:
Gonzalo, J., Domínguez, D., García-Gutiérrez, A., & Escapa, A. (2020).
On the development of a parametric aerodynamic model of a stratospheric airship. Aerospace Science and Technology, 107, 106316.

of this paper, bi-symmetric fins ease the interface between thin and thick panels. The fin definition is then reduced to leading edge position and sweep angle, fin span, tip chord and trailing edge sweep angle (Figure 18, left). The aerofoils are considered symmetric and hence flat thin panels are used.

Special attention must be paid to the attachment of thin and thick panels [28], [32]. Although they may share vertexes, the calculation of perturbation velocities proposed in eq. (15) requires knowledge of the neighbour relationships. The results in [17] may infer that not having the exact same attachment vertex between thick and thin panels (including wakes) requires higher order singularity distributions to produce reliable estimates. In this study, this problem is avoided by defining a dedicated mesh where thin and think panels always share vertexes.

For both thin and thick panels, once attached, the neighbours change (Figure 7). In order to homogenise calculations, all thin and thick panels are converted into generic panels. Thus, thick panels are almost unchanged whereas thin ones are doubled into upper and lower panels, each one retaining the potential induced by the rest of the panels, plus or minus half of its own influence. The neighbourhood relationships need to be re-established to generate a structure where numeric derivation of doublets is simple from the geometric point of view. An expedient way to cut neighbour connections is to duplicate vertices in the same space position, so that one panels does not see other as neighbour because it does not share the vertex (see thick panels on the right side of Figure 7).

Please, cite as:
Gonzalo, J., Domínguez, D., García-Gutiérrez, A., & Escapa, A. (2020).
On the development of a parametric aerodynamic model of a stratospheric airship. Aerospace Science and Technology, 107, 106316.

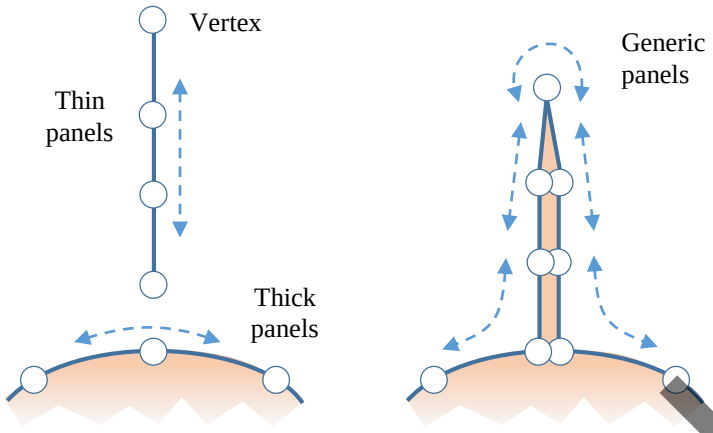

Figure 7: Attachment of thin and thick panels (dotted line show neighbourhood relationship).

The whole panel set is divided into patches. The number of panels in each patch is controlled by two figures, one for the north-south direction and the other for the west-east one (Figure 8). From that geometry, wakes are attached at trailing edges with a parametric definition concerning the number of panels and their characteristic individual length.

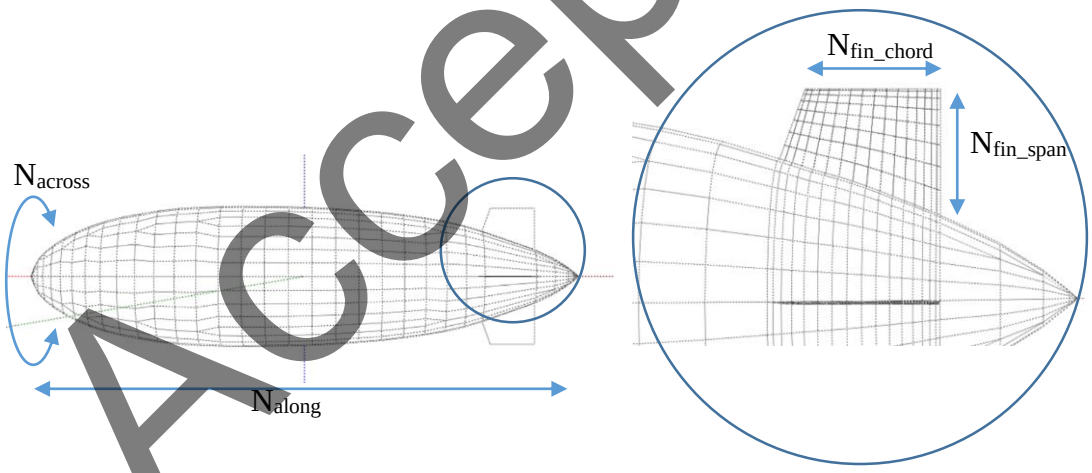

Figure 8: Definition of number of panels.

Operational conditions are defined by the velocity vector, normally given by its modulus, the angle of attack and the angle of sideslip.

Please, cite as:
Gonzalo, J., Domínguez, D., García-Gutiérrez, A., & Escapa, A. (2020).
On the development of a parametric aerodynamic model of a stratospheric airship. Aerospace Science and Technology, 107, 106316.

3. Code validation

The validation is performed in two steps: these involve applying thick panels in blunt bodies and thin panels in short wings. The interaction of thick and thin panels will be later considered in a real experiment in a wind tunnel.

3.1. Thick panels

Thick panels are validated using the well-known potential solution for revolution ellipsoids [34]. The fineness ratio (FR) is defined as the division of the major axis into the minor one (Figure 9). The ellipsoids are shapes similar to the ones used in airships, where revolution forms help from the structural point of view. In thick panels, Dirichlet boundary conditions are applied to force a prescribed interior potential.

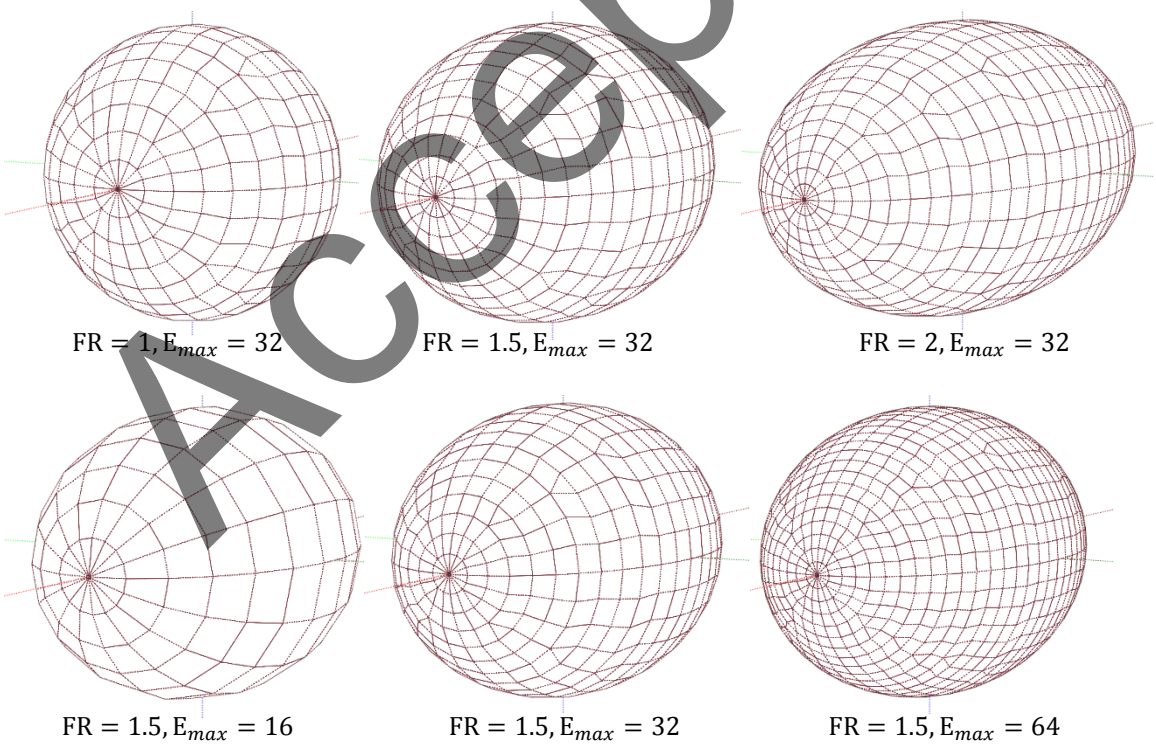

Figure 9: Representation of ellipsoid with different fineness ratio and panels in central belt.

Please, cite as:
Gonzalo, J., Domínguez, D., García-Gutiérrez, A., & Escapa, A. (2020).
On the development of a parametric aerodynamic model of a stratospheric airship. Aerospace Science and Technology, 107, 106316.

The number of panels to define the ellipsoid should be carefully selected as the difference in maximum and minimum radii may be important. A constant number in the azimuthal direction could lead to a very widespread in the panel area distribution, which is not convenient from the numerical point of view. Construction techniques explained in §2.6 have been adopted to optimise the panel distribution, producing test meshes such as the ones shown in Figure 9. Triangular panels are used to increase/decrease the panels in a transversal band when radius is much higher than former strip.

The results of solving the equations for source/doublet distribution, the interpolation for surface tangential velocity and the conversion into pressure coefficients, provides final figures as sketched in Figure 10 and detailed in Figure 11 for different fineness ratios. The results are compared to those provided by theory with an excellent level of matching even for a relatively low number of panels (and only 100 milliseconds executing time in a conventional processor). Besides, D'Alembert paradox is met for every angle of attack tested.

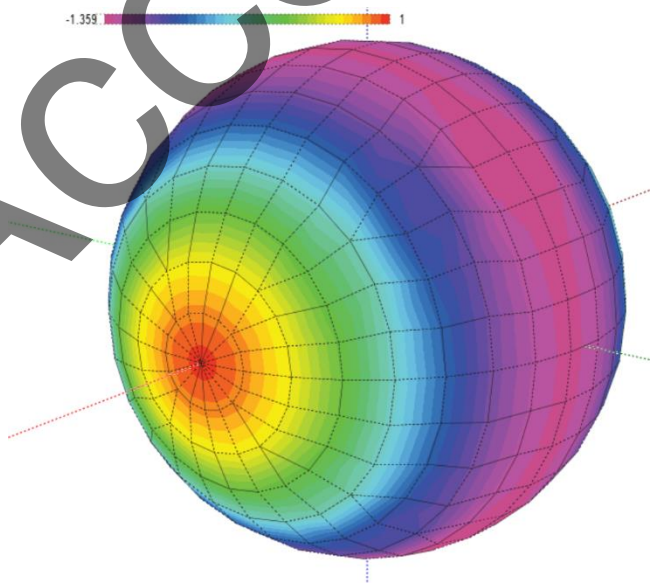

Figure 10: Pressure distribution on a sphere in a uniform flow.

Please, cite as:
Gonzalo, J., Domínguez, D., García-Gutiérrez, A., & Escapa, A. (2020).
On the development of a parametric aerodynamic model of a stratospheric airship. Aerospace Science and Technology, 107, 106316.

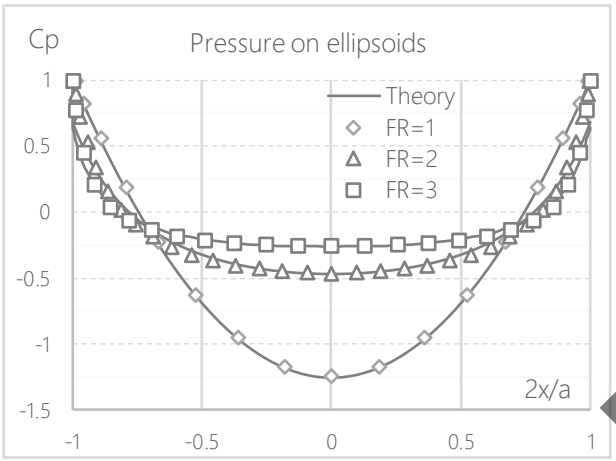

Figure 11: Pressure coefficients on ellipsoids of different fineness ratios.

When angles of attack are imposed, theoretic results are also perfectly achieved [35]. Furthermore, experimental results are available in the same reference, as shown in Figure 12, for a fineness ratio of 2 and a very large angle of attack of 20 degrees. The upper central line of the ellipsoid presents a suction area which is perfectly reproduced by the panel method in most of the hull. In the lower central line, only one third of the curve is followed accurately. The source of the misalignment is related to viscid effects; the widening of the boundary layer and eventual separation limits the ideal under-pressure produced by velocity at the leeward side. In order to capture this effect, an extra panel sheet modelling the separation layer would be necessary [34], [36], but this is out of the scope of this research. Figure 12 is a good representation of the inherent qualities and limitations of the panel method for blunt bodies.

Please, cite as:
Gonzalo, J., Domínguez, D., García-Gutiérrez, A., & Escapa, A. (2020).
On the development of a parametric aerodynamic model of a stratospheric airship. Aerospace Science and Technology, 107, 106316.

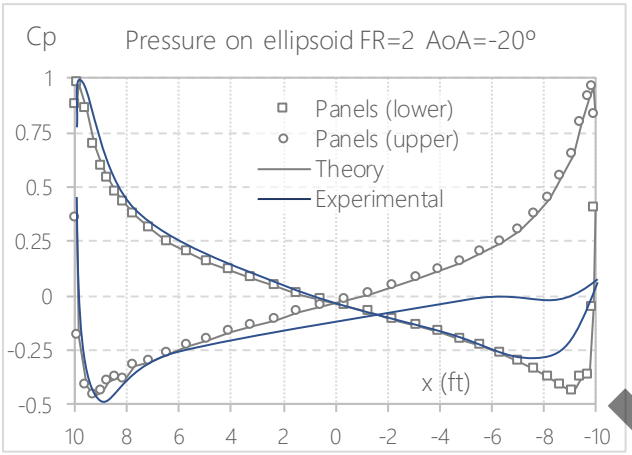

Figure 12: Pressure on a 20-ft, FR=2 ellipsoid with 20 degrees angle of attack (panels, theory and experimental [34]).

3.2. Thin panels

The validation of the panel method implementing thin elements (no sources, Neumann boundary conditions on them) is carried out using flat rectangular wings of little aspect ratio. These surfaces are similar to the fins implemented in most airships.

In general, the results need to be compared to potential solutions already reported in the literature. The lifting line theory of Prandtl [37] and the solving method implemented by Multhopp [38] provide good validation data. Figure 13 shows a typical distribution of pressure coefficients on the wing and the associated wake; in this case, a rectangular flat wing of aspect ratio 4 is flying with angle of attack 5-deg with a straight wake to ease comparison. As explained above (§2.6), the panel geometry is configured following a cosine law in the along and across flight direction, in a way that pressure changes at leading edge and wing tips are more accurately captured (more details in [37]). The number of panels in each direction is selectable and, for total figures lower than 128×128 the computing time is in the order of few seconds with conventional desktop hardware without any parallelisation effort.

Please, cite as:
Gonzalo, J., Domínguez, D., García-Gutiérrez, A., & Escapa, A. (2020).
On the development of a parametric aerodynamic model of a stratospheric airship. Aerospace Science and Technology, 107, 106316.

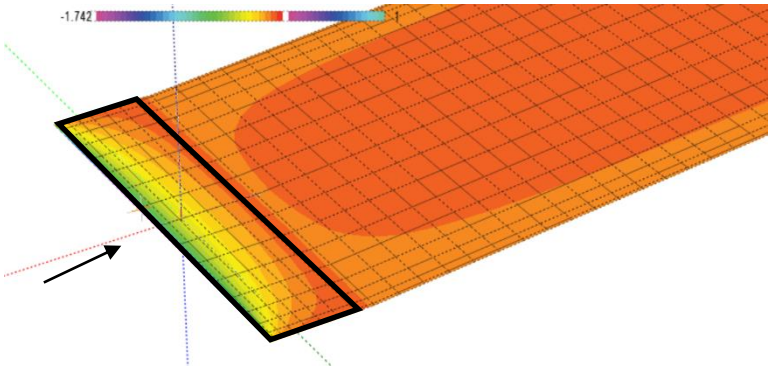

Figure 13: Pressure coefficient on a flat wing AR=4, AoA=5 degrees.

The lift coefficient, as presented in Figure 14, perfectly matches the literature reference for this particular aspect ratio up to an angle of attack of 15 degrees. Further incidence angles produce a loss of linearity that the panel method slightly underestimates.

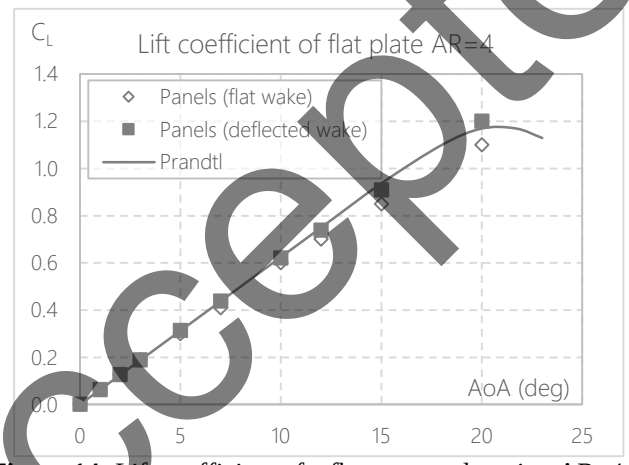

Figure 14: Lift coefficient of a flat rectangular wing AR=4.

The pressure distribution in the thin airfoil (chordwise) is shown in Figure 15 for two angles of attack within the linear range in a very large aspect ratio wing. Again, the results fully meet those of thin airfoil theory and the analytic solution given in [36] for bidimensional flat plates. The well-known suction peak in the upper side of the leading edge is reasonably well captured (the reader should note the logarithmic scale of ordinate axis in the plot).

Please, cite as:
Gonzalo, J., Domínguez, D., García-Gutiérrez, A., & Escapa, A. (2020).
On the development of a parametric aerodynamic model of a stratospheric airship. Aerospace Science and Technology, 107, 106316.

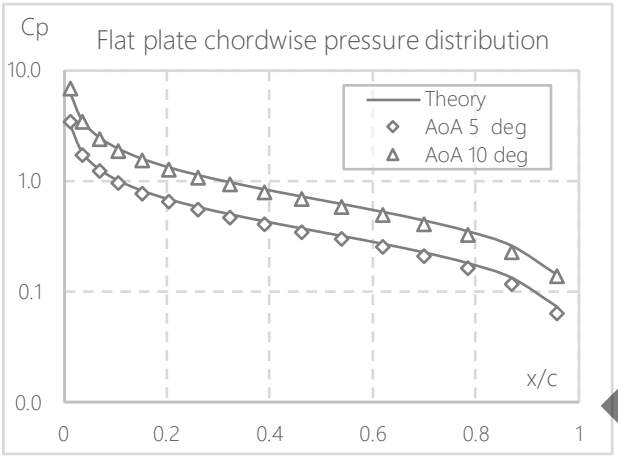

Figure 15: Pressure coefficient on a flat wing in 2D, AoA 5 degrees and 10 degrees.

To validate the lift spanwise distribution, a Multhopp [37] solution has been implemented using 301 nodes spanwise in a rectangular wing. Figure 16 shows high levels of agreement when comparing the results of the panel method to that of the lifting line theory. In this case it is more important to capture pressure changes close to the wing tips, where the panels should have a lower size. As these panels have also associated trailing wakes, the impact in the processing time is more striking.

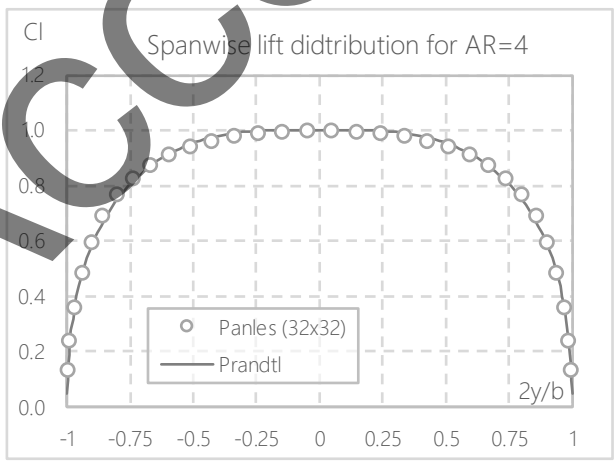

Figure 16: Spanwise lift distribution for a flat plate AoA 5 degrees, AR=4.

Comparing along and across flight pressure distributions (Figure 15 and Figure 16), it can be justified that relatively more panels are needed chordwise due to the strong variation of pressure in the first quarter of the chord. To have a good estimation of the effect of the number

Please, cite as:
Gonzalo, J., Domínguez, D., García-Gutiérrez, A., & Escapa, A. (2020).
On the development of a parametric aerodynamic model of a stratospheric airship. Aerospace Science and Technology, 107, 106316.

of panels in the results, Figure 17 has been prepared to calculate the lift coefficient using different combinations of panel numbers in the two chord/span directions. Knowing that the result should be around 0.31, the only configurations meeting a reasonably good result (±5%) are marked in dark. They correspond to 16 or more panels spanwise but at least 32 chordwise. A safe 32×64 grid provides acceptable results in all tests developed in this study.

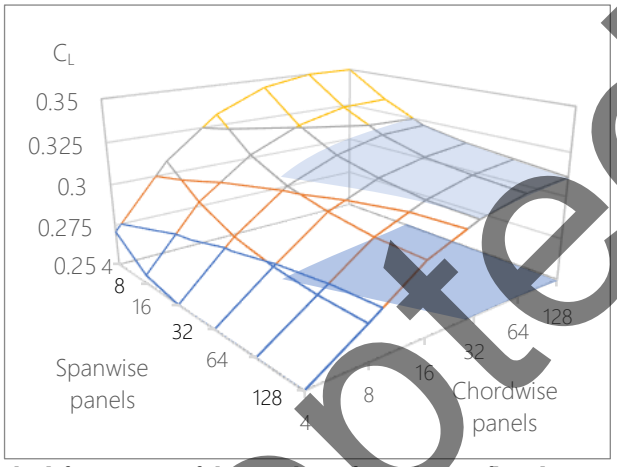

Figure 17: Effect in the lift estimate of the number of panels in a flat plate AoA 5 degrees, AR=4.

When considering other values for the aspect ratio, the lift coefficient is changed due to tip (and wake) vortex shedding. The results can be seen in Figure 18 for an angle of attack of 5 degrees. As expected, when aspect ratio increases, the bidimensional solution ($c_l = 2\pi \cdot AoA$) is approached progressively.

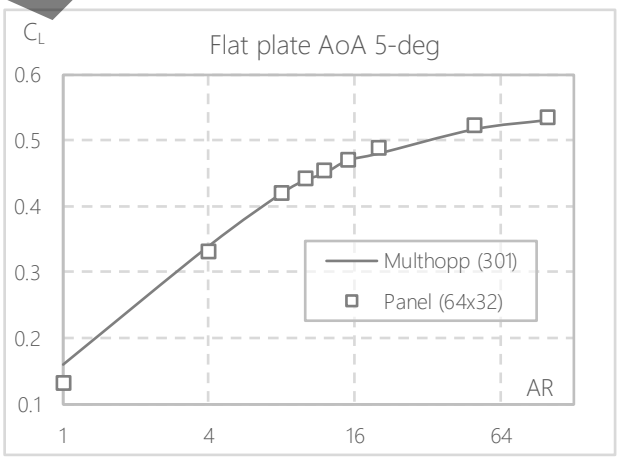

Figure 18: Lift coefficient for a flat plate AoA 5 degrees for wing different aspect ratios.

Please, cite as:
Gonzalo, J., Domínguez, D., García-Gutiérrez, A., & Escapa, A. (2020).
On the development of a parametric aerodynamic model of a stratospheric airship. Aerospace Science and Technology, 107, 106316.

4. Airship application results

For the tests, a classical Gertler 4154 Series 58 revolution body [39] has been used, with the following definition (Figure 18):

$$\eta^2 = a_1\xi + a_2\xi^2 + a_3\xi^3 + a_4\xi^4 + a_5\xi^5 + a_{16}\xi^6, \quad (22)$$

where $\xi = x/L$ and $\eta = r/D$, being L the length of the hull and D the maximum diameter. In this particular case the fineness ratio L/D is 4. The a_i coefficients can be extracted from [39], resulting $a_1 = 1.000000$, $a_2 = 2.149653$, $a_3 = -17.773496$, $a_4 = 36.716580$, $a_5 = -33.511285$ and $a_6 = 11.418548$.

For the experimental tests, a 1 meter length model has been manufactured (Figure 19, right). Although the size of the real model is undisclosed, the experiment is prepared to replicate performance at length-based Reynolds about 10^6, as expected in stratospheric HAPS [1].

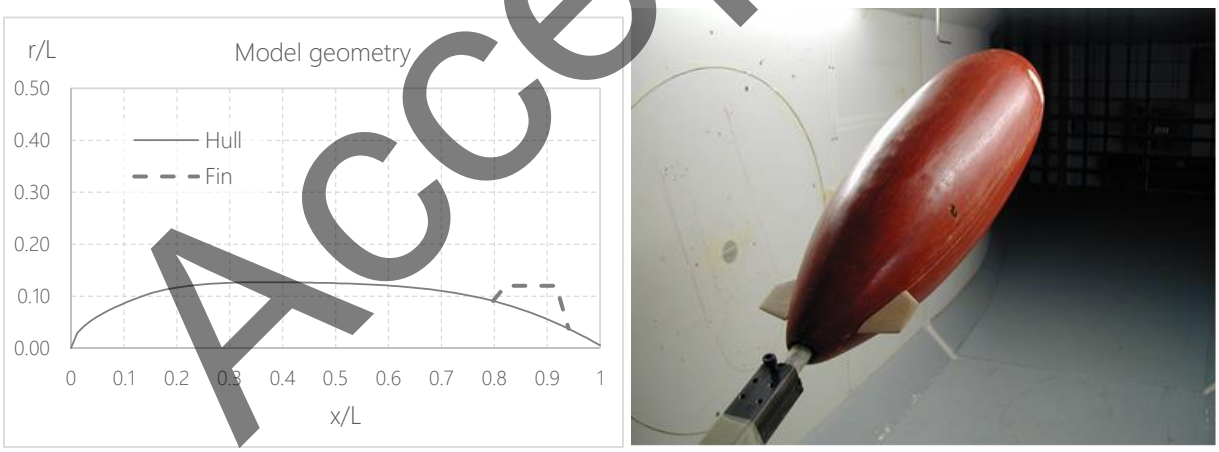

Figure 19: Geometry of test model and picture in wind tunnel.

Accepting that drag coefficients are out of the scope of pure potential codes, as is the case here, the most promising results are those related to lift and pitch moments. Considering symmetry, the same results are applicable to lateral forces and yaw moments when the angle of attack is substituted by the angle of sideslip. Experimental tests were prepared to obtain two

Please, cite as:
Gonzalo, J., Domínguez, D., García-Gutiérrez, A., & Escapa, A. (2020).
On the development of a parametric aerodynamic model of a stratospheric airship. Aerospace Science and Technology, 107, 106316.

sets of useful data: pressure distributions along the hull gores and the moments measured by a precision balance.

The corresponding numerical test grid was prepared with 64×64 panels in the main hull, 32 chordwise and 16 spanwise in fins and 15 panel length wake from every trailing edge thin panel. Executions were repeated until the wake stabilisation (typically four iterations). Processing time is in the order of 1 minute. The pressure coefficients, as shown in Figure 20, were integrated to obtain force and moment coefficients. This integration is developed individually for all active patches, and moments properly moved before being accumulated into total values.

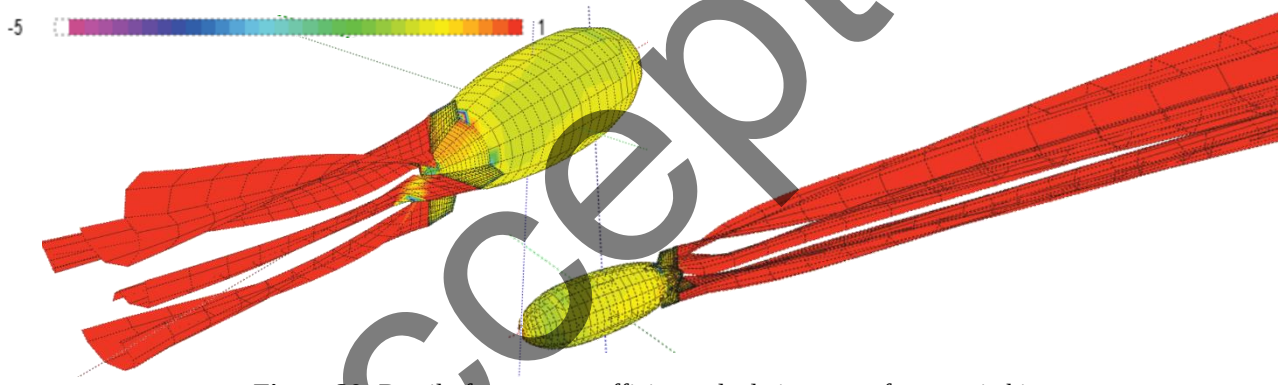

Figure 20: Detail of pressure coefficient calculations on reference airship.

Pressure profiles are estimated and measured for zero, moderate (9 degrees) and large (18 degrees) angles of attack. The measurement is taken following along-hull lines at 0 degrees (symmetry plane, downwards), 90 degrees (side) and 180 degrees (symmetry plane, upwards).

Figure 21 represents the pressure profile given by the panel method in the airship bi-symmetric position, rotation axis being parallel to freestream. The estimations are perfectly compatible with the measurements taken in the wind tunnel. In the leading surface of the hull, the method slightly underestimates the experimental values. However, the mismatch may be

Please, cite as:
Gonzalo, J., Domínguez, D., García-Gutiérrez, A., & Escapa, A. (2020).
On the development of a parametric aerodynamic model of a stratospheric airship. Aerospace Science and Technology, 107, 106316.

due to the inaccuracies in the position of the pressure probes within the model, where manual manufacturing is not perfect. In the trailing panels the measurement dispersion is higher but still very close to the numerical results.

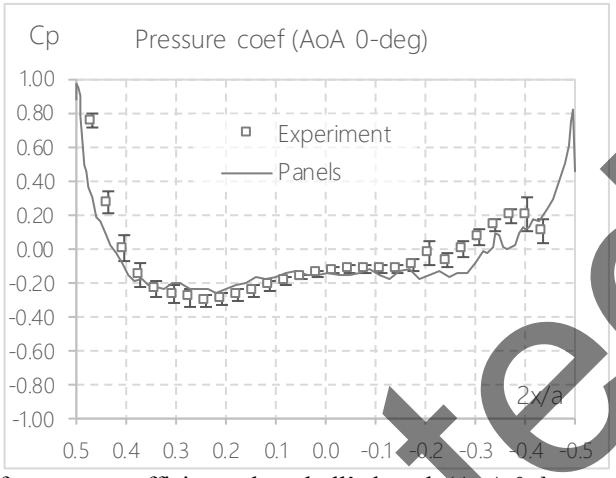

Figure 21: Detail of pressure coefficients along hull's length (AoA 0 degrees, 8 gores averaged).

As the angle of attack increases to 9 degrees (same could be said for the sideslip angle in this type of vehicles) the differences widen in the back area due to incipient flow detachment (Figure 22). This effect, although relevant to the plot, affects regions of poor contribution to the global lift and moment given the typical pressure values and the involved area. On the contrary, drag estimations are inaccurate due to these artefacts. With respect to the leading region, only the bottom area is slightly underestimated. There is no evident reason for that. In fact, potential theory results are more likely correct as shown in the ellipsoid case.

Please, cite as:
Gonzalo, J., Domínguez, D., García-Gutiérrez, A., & Escapa, A. (2020).
On the development of a parametric aerodynamic model of a stratospheric airship. Aerospace Science and Technology, 107, 106316.

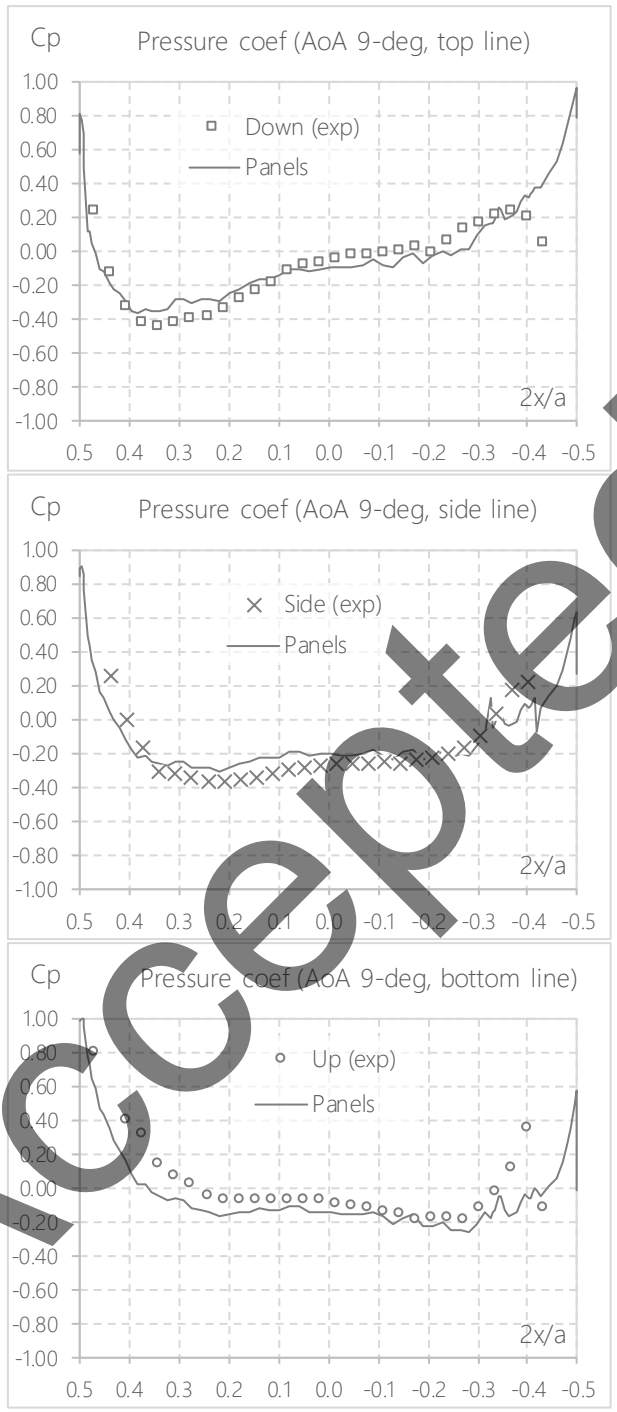

Figure 22: Detail of pressure coefficients along hull's length (AoA 9 degrees).

Finally, for a large angle of attack (18 degrees depicted in Figure 23) the numeric method acceptably matches the experimental results with the same exceptions of the trailing region. The rest of the profile is close to tunnel measurements. As far as it is known, high altitude

Please, cite as:
Gonzalo, J., Domínguez, D., García-Gutiérrez, A., & Escapa, A. (2020).
On the development of a parametric aerodynamic model of a stratospheric airship. Aerospace Science and Technology, 107, 106316.

platforms will rarely fly with large angles of attach or sideslip in nominal operations. In any case, for other flight conditions, the detachment of body boundary layer and its effect on fins (both stability and control) needs to be investigated in detail for these parametric models. The use of extra wakes starting on thick panel boundaries is a promising technique (as in [17]).

Please, cite as:
Gonzalo, J., Domínguez, D., García-Gutiérrez, A., & Escapa, A. (2020).
On the development of a parametric aerodynamic model of a stratospheric airship. Aerospace Science and Technology, 107, 106316.

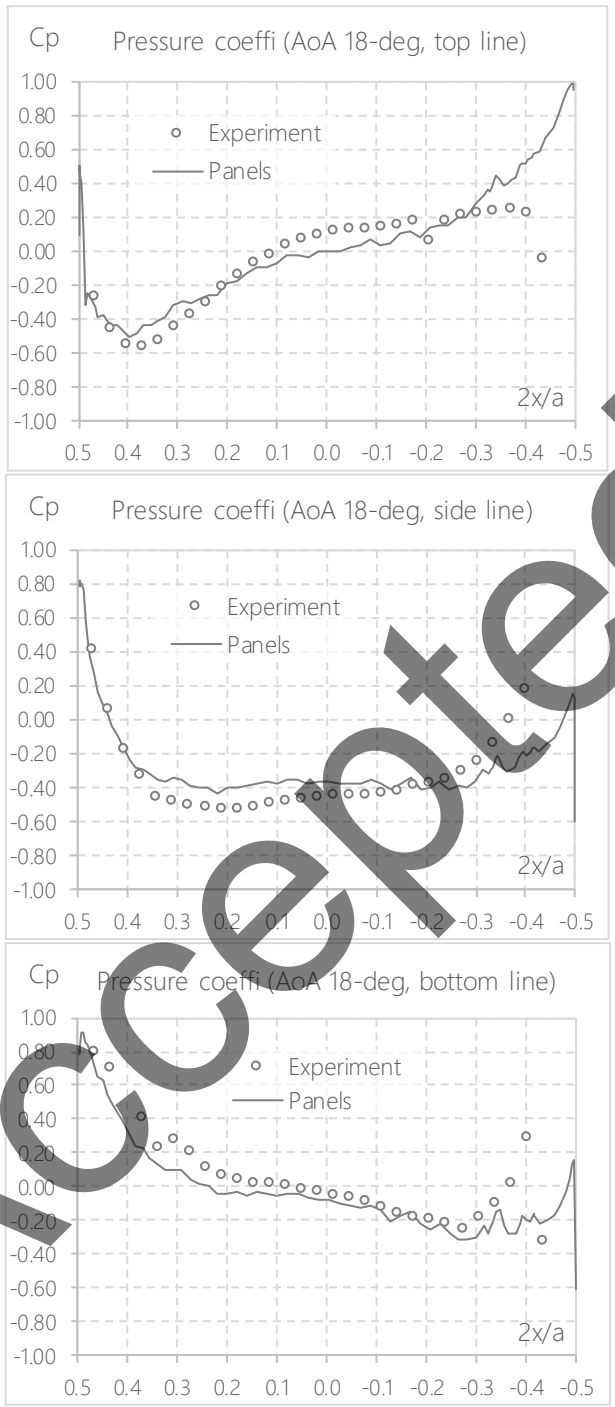

Figure 23: Detail of pressure coefficients along hull's length (AoA 18 degrees).

As a validation of most representative integrated coefficients, Figure 24 shows the comparison between the pitch moments with respect to the vehicle centre from several angles of attack. The test includes the bare hull and the fin-equipped vehicle. Since those moments

Please, cite as:
Gonzalo, J., Domínguez, D., García-Gutiérrez, A., & Escapa, A. (2020).
On the development of a parametric aerodynamic model of a stratospheric airship. Aerospace Science and Technology, 107, 106316.

are less dependent on the minor deviations of the pressure curves in certain areas, the matching is very good. Only with extreme angles of attack does the potential method slightly underestimates the moment, probably because the high-pressure area around the trailing stagnation point vanishes in real conditions due to viscosity swept and detachment.

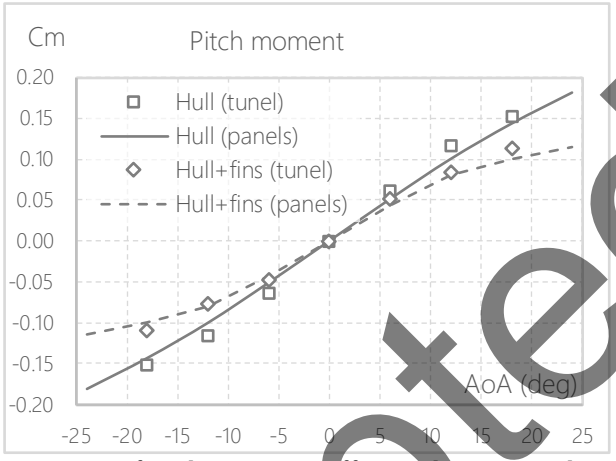

Figure 24: Comparison of pitch moment coefficients between airship and bare hull.

The pressures can be integrated quasi-circumferentially along the hull to produce plots such as those in Figure 25 and Figure 26 for vertical and horizontal forces. Whereas the first provide net lift only in the case of fins installed, the second integrates to almost zero as induced drag from fins is negligible with respect to the whole body. Both distributions are in any case valuable to support fabric load estimations and position of instruments.

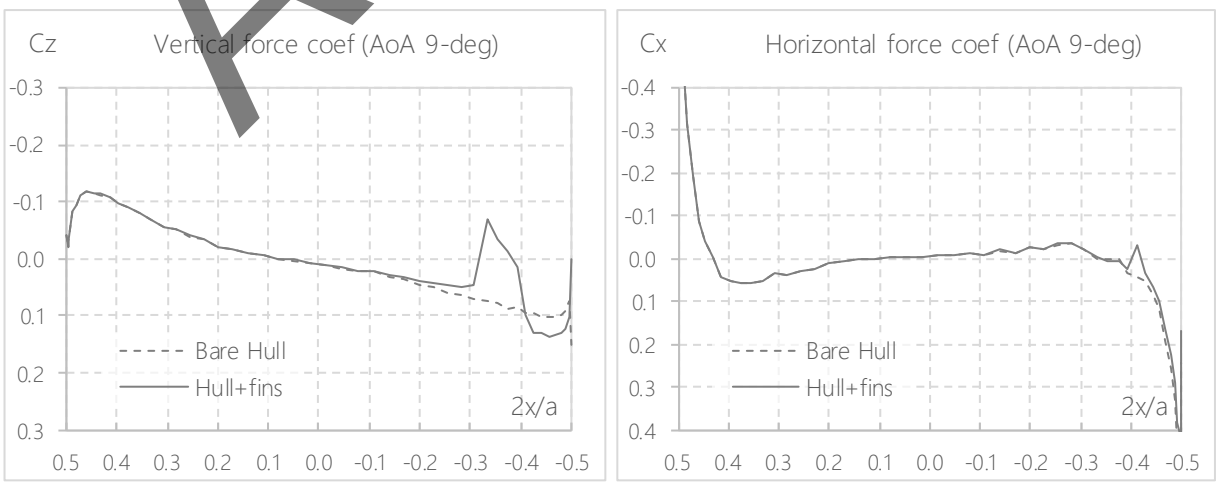

Figure 25: Z-axis and X-axis force coefficients along the airship hull for AoA 9-deg.

Please, cite as:
Gonzalo, J., Domínguez, D., García-Gutiérrez, A., & Escapa, A. (2020).
On the development of a parametric aerodynamic model of a stratospheric airship. Aerospace Science and Technology, 107, 106316.

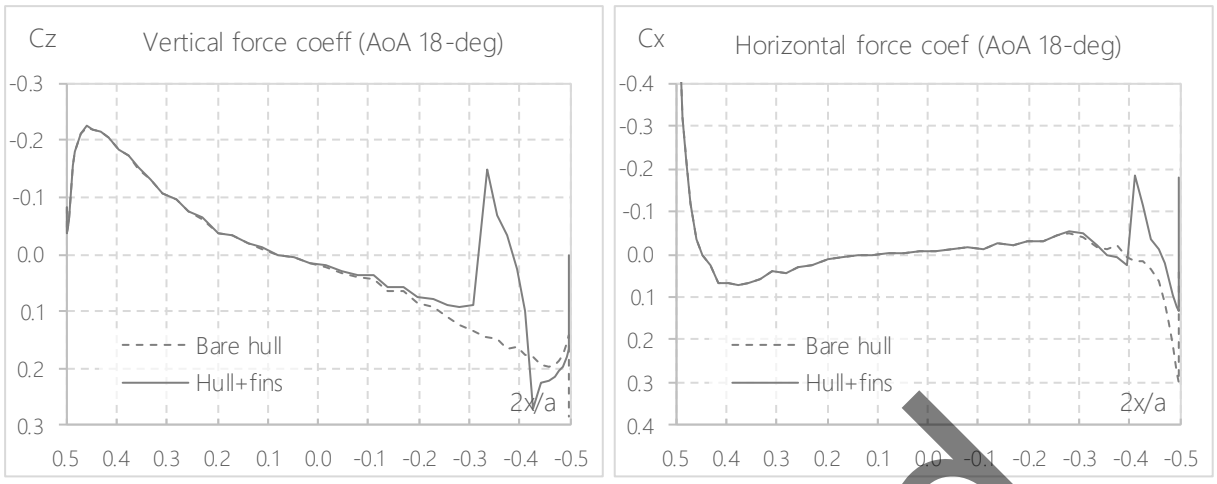

Figure 26: Z-axis and X-axis force coefficients along the airship hull for AoA 18-deg.

5. Conclusions

Although the usage of panel methods for the preliminary estimation of aerodynamic parameters is extensively used in aerofoil characterisation, the difficulty of preparing 3D geometries for airships very often leads engineers to move directly to throughput-expensive CFD models.

This paper shows a panel method, thus a potential flow solver, specifically developed for the modelling of conventional airships models whose geometry is defined from a simple parameter set. Thick and thin panels are used together with wake discontinuity surfaces forcing the Kutta condition to be met at trailing segments. The definition of those elements is prepared to simplify the interaction among them so that user intervention is at a minimum. The mesh generation already improves granularity in the regions where pressures present larger gradients. Besides, detached wakes from trailing edges are automatically generated and iteratively evolved to follow local velocity conditions.

Results of using thick and thin panels have been validated independently by using well-characterised objects such as ellipsoids (similar to typical hulls) and flat short rectangular

Please, cite as:
Gonzalo, J., Domínguez, D., García-Gutiérrez, A., & Escapa, A. (2020).
On the development of a parametric aerodynamic model of a stratospheric airship. Aerospace Science and Technology, 107, 106316.

wings (similar to typical fins) respectively. Later, the combination of these have been successfully tested for a real airship design against wind tunnel measurements. The results are acceptable given the limitations of the potential theory, with the advantage of development time and computer requirements.

Similarly, as with aerofoils, the results of this method may be considered as the starting point of other studies to add boundary layer effects such as laminar-turbulent transition or models of detached structures changing the windfield configuration. The method enables the deployment of wake discontinuity surfaces not only from thin fin panels but also from those thick panels where the pressure coefficient and its gradient meet certain conditions. The three-dimensional characteristics of the airship adds complexity to these issues but the agility of the method makes it convenient for preliminary estimation or iterative optimisation processes.

Acknowledgements

We are grateful to the referees for their useful and constructive revision that has enhanced the manuscript. Authors would like to acknowledge Instituto de Microgravedad Ignacio da Riva, and in particular its director Dr. Ángel Sanz for the support in the development of the experimental tests in this article.

Annex: Basics of panel method formulation

- Panel geometry

Principles of panel methods are mainly borrowed from [40] and [30]. Being those comprehensive references and with particular nomenclature, this annex consolidates the basic concepts with a more detailed nomenclature and a direct connection with the article for reproducibility. Minor errors in references have been corrected as well (e.g. 10.107/9 of [30]).

Please, cite as:
Gonzalo, J., Domínguez, D., García-Gutiérrez, A., & Escapa, A. (2020).
On the development of a parametric aerodynamic model of a stratospheric airship. Aerospace Science and Technology, 107, 106316.

A generic quadrilateral panel is shown in Figure 27, with corners located at $\bar{x}^B_{1..4}$ in platform's body frame. If the panel is flat, the centroid can be calculated by averaging the coordinates of the corners. This procedure can also be used to estimate the centre in the case the rectilinear panel is not completely flat. From this reference points, a panel local reference P frame is constructed using the panel normal as z^P axis. The panel x^P axis is typically selected in the direction of the object's body x axis (flight direction). The phasors of local frame can be written as:

$$\bar{k}^B = \frac{(\bar{x}_1^B - \bar{x}_3^B) \wedge (\bar{x}_2^B - \bar{x}_4^B)}{|(\bar{x}_1^B - \bar{x}_3^B) \wedge (\bar{x}_2^B - \bar{x}_4^B)|}, \qquad \bar{j}^B = \frac{\bar{x}_1^B + \bar{x}_2^B - \bar{x}_3^B - \bar{x}_4^B}{|\bar{x}_1^B + \bar{x}_2^B - \bar{x}_3^B - \bar{x}_4^B|}, \qquad \bar{\imath}^B = \bar{j}^B \wedge \bar{k}^B. \tag{23}$$

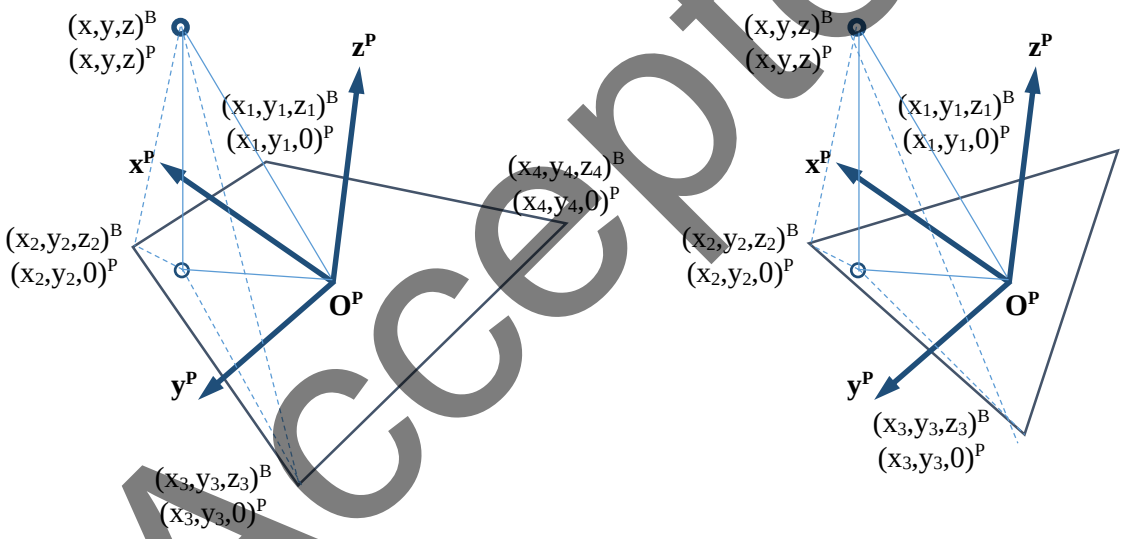

Figure 27: Quadrilateral and triangular panel geometries.

The vector product in the first formula also serves to calculate the surface of the panel by adding the area of the two triangles. The rotation matrixes to convert vector from B to P frames and vice-versa are:

$$\bar{x}^B = L_{PB}\bar{x}^B, \qquad L_{PB} = \begin{bmatrix} \bar{\imath}_x^B & \bar{\imath}_y^B & \bar{\imath}_x^B \\ \bar{j}_x^B & \bar{j}_y^B & \bar{j}_z^B \\ \bar{k}_x^B & \bar{k}_y^B & \bar{k}_z^B \end{bmatrix}, \tag{24}$$

Please, cite as:
Gonzalo, J., Domínguez, D., García-Gutiérrez, A., & Escapa, A. (2020).
On the development of a parametric aerodynamic model of a stratospheric airship. Aerospace Science and Technology, 107, 106316.

$$\bar{x}^P = L_{BP}\bar{x}^B, \qquad L_{BP} = L_{PB}^T. \tag{25}$$

The positions of the flat panel corners shall, when converted to panel frame coordinates, have a null third coordinate.

Other geometric variables to be used in the calculation of influence parameters in this paper are:

$$\bar{d}_{12} = \bar{x}_2 - \bar{x}_1, \qquad \bar{d}_{23} = \bar{x}_3 - \bar{x}_2, \qquad \bar{d}_{34} = \bar{x}_4 - \bar{x}_3, \qquad \bar{d}_{41} = \bar{x}_1 - \bar{x}_4,$$

$$d_{12} = \sqrt{(x_2 - x_1)^2 + (y_2 - y_1)^2}, \qquad d_{23} = \sqrt{(x_3 - x_2)^2 + (y_3 - y_2)^2},$$

$$d_{34} = \sqrt{(x_4 - x_3)^2 + (y_4 - y_3)^2}, \qquad d_{41} = \sqrt{(x_1 - x_4)^2 + (y_1 - y_4)^2}, \tag{26}$$

$$m_{12} = \frac{y_2 - y_1}{x_2 - x_1}, \qquad m_{23} = \frac{y_3 - y_2}{x_2 - x_2}, \qquad m_{34} = \frac{y_4 - y_3}{x_4 - x_3}, \qquad m_{41} = \frac{y_1 - y_4}{x_1 - x_4}, \tag{27}$$

$$e_1 = (x - x_1)^2 + z^2, \qquad e_2 = (x - x_2)^2 + z^2,$$

$$e_3 = (x - x_3)^2 + z^2, \qquad e_4 = (x - x_4)^2 + z^2, \tag{28}$$

$$r_1 = \sqrt{e_1 + (y - y_1)^2}, \qquad r_2 = \sqrt{e_2 + (y - y_2)^2},$$

$$r_3 = \sqrt{e_3 + (y - y_3)^2}, \qquad r_4 = \sqrt{e_4 + (y - y_4)^2}, \tag{29}$$

$$h_1 = (x - x_1)(y - y_1), \qquad h_2 = (x - x_2)(y - y_2),$$

$$h_3 = (x - x_3)(y - y_3), \qquad h_4 = (x - x_4)(y - y_4). \tag{30}$$

The extension of the above formulation to triangular panes it is performed by removing references to corner 4 and considering the connection between number 3 and 1.

Please, cite as:
Gonzalo, J., Domínguez, D., García-Gutiérrez, A., & Escapa, A. (2020).
On the development of a parametric aerodynamic model of a stratospheric airship. Aerospace Science and Technology, 107, 106316.

- Source uniform distribution

The potential induced by a constant source ($\emptyset_S$) distributed along and across a panel, the cause, in a generic point (x, y, z), the effect, is:

$$\emptyset_S(x,y,z) = -\frac{\sigma}{4\pi}\int_\Sigma \frac{d\xi d\eta}{\sqrt{(x-\xi)^2+(y-\eta)^2+z^2}}, \tag{31}$$

where ξ and η are the coordinates of the differential source being integrated. Following mathematics of [40], the exact formulation for rectilinear borders (Figure 27) leads to:

$$\emptyset_S = -\frac{\sigma}{4\pi}\left[\frac{(x-x_1)(y_2-y_1)-(y-y_1)(x_2-x_1)}{d_{12}}\ln\frac{r_1+r_2+d_{12}}{r_1+r_2-d_{12}} + \frac{(x-x_2)(y_3-y_2)-(y-y_2)(x_3-x_2)}{d_{23}}\ln\frac{r_2+r_3+d_{23}}{r_2+r_3-d_{23}} + \right.$$

$$\left. + \frac{(x-x_3)(y_4-y_3)-(y-y_3)(x_4-x_3)}{d_{34}}\ln\frac{r_3+r_4+d_{34}}{r_3+r_4-d_{34}} + \frac{(x-x_4)(y_1-y_4)-(y-y_4)(x_1-x_4)}{d_{41}}\ln\frac{r_4+r_1+d_{41}}{r_4+r_1-d_{41}}\right] +$$

$$+|z|w_S, \tag{32}$$

where w is the velocity component along the panel normal (z axis), given by:

$$w_S = \frac{\sigma}{4\pi}\left[\tan^{-1}\left(\frac{m_{12}e_1-h_1}{zr_1}\right) - \tan^{-1}\left(\frac{m_{12}e_2-h_2}{zr_2}\right) + \tan^{-1}\left(\frac{m_{23}e_2-h_2}{zr_2}\right) - \tan^{-1}\left(\frac{m_{23}e_3-h_3}{zr_3}\right)\right.$$

$$\left. + \tan^{-1}\left(\frac{m_{34}e_3-h_3}{zr_3}\right) - \tan^{-1}\left(\frac{m_{34}e_4-h_4}{zr_4}\right) + \tan^{-1}\left(\frac{m_{41}e_4-h_4}{zr_4}\right) - \tan^{-1}\left(\frac{m_{41}e_1-h_1}{zr_1}\right)\right]. \tag{33}$$

The potential is defined throughout the domain but it presents a discontinuity in the surface of the panel, where:

$$w_S(z=\pm 0) = \frac{\partial \emptyset_S}{\partial n} = \pm\frac{1}{2}\sigma. \tag{34}$$

Please, cite as:
Gonzalo, J., Domínguez, D., García-Gutiérrez, A., & Escapa, A. (2020).
On the development of a parametric aerodynamic model of a stratospheric airship. Aerospace Science and Technology, 107, 106316.

Outside the panel, w_S is null as intuitively corresponds to source panel in the same plane. Although w_S is part of the $\emptyset_S$ formula, the $|z|$ term closes to null at the panel in both sides, and hence continuity is ensured.

The other two components of the velocity, always in local coordinates, are:

$$u_S = \frac{\sigma}{4\pi}\left[\frac{(y_2-y_1)}{d_{12}}\ln\frac{r_1+r_2-d_{12}}{r_1+r_2+d_{12}} + \frac{(y_3-y_2)}{d_{23}}\ln\frac{r_2+r_3-d_{23}}{r_2+r_3+d_{23}} + \right.$$

$$\left. + \frac{(y_4-y_3)}{d_{34}}\ln\frac{r_3+r_4-d_{34}}{r_3+r_4+d_{34}} + \frac{(y_1-y_4)}{d_{41}}\ln\frac{r_4+r_1-d_{41}}{r_4+r_1+d_{41}}\right], \quad (35)$$

$$v_S = \frac{\sigma}{4\pi}\left[\frac{(x_2-x_1)}{d_{12}}\ln\frac{r_1+r_2-d_{12}}{r_1+r_2+d_{12}} + \frac{(x_3-x_2)}{d_{23}}\ln\frac{r_2+r_3-d_{23}}{r_2+r_3+d_{23}} + \right.$$

$$\left. + \frac{(x_4-x_3)}{d_{34}}\ln\frac{r_3+r_4-d_{34}}{r_3+r_4+d_{34}} + \frac{(x_1-x_4)}{d_{41}}\ln\frac{r_4+r_1-d_{41}}{r_4+r_1+d_{41}}\right]. \quad (36)$$

- Doublet uniform distribution

In an analogous manner, the potential induced by a constant doublet ($\emptyset_D$) distributed along and across a panel, the cause, in a generic point (x, y, z), the effect, is:

$$\emptyset_D(x,y,z) = -\frac{\mu}{4\pi}\int_\Sigma \frac{z\, d\xi d\eta}{[(x-\xi)^2+(y-\eta)^2+z^2]^{3/2}}. \quad (37)$$

The formulation [40] for rectilinear borders (Figure 27) leads to:

$$\emptyset_D = \frac{\sigma}{4\pi}\left[\tan^{-1}\left(\frac{m_{12}e_1-h_1}{zr_1}\right) - \tan^{-1}\left(\frac{m_{12}e_2-h_2}{zr_2}\right) + \tan^{-1}\left(\frac{m_{23}e_2-h_2}{zr_2}\right) \right.$$

$$\left. - \tan^{-1}\left(\frac{m_{23}e_3-h_3}{zr_3}\right) \right.$$

$$\left. + \tan^{-1}\left(\frac{m_{34}e_3-h_3}{zr_3}\right) - \tan^{-1}\left(\frac{m_{34}e_4-h_4}{zr_4}\right) + \tan^{-1}\left(\frac{m_{41}e_4-h_4}{zr_4}\right) - \tan^{-1}\left(\frac{m_{41}e_1-h_1}{zr_1}\right)\right]. \quad (38)$$

Please, cite as:
Gonzalo, J., Domínguez, D., García-Gutiérrez, A., & Escapa, A. (2020).
On the development of a parametric aerodynamic model of a stratospheric airship. Aerospace Science and Technology, 107, 106316.

As it occurred before with the normal component of velocity of a source panel, now the potential induced by the doublet distribution shows a discontinuity in the two sides of the panel:

$$\emptyset_D(z = 0 \pm) = \pm\frac{1}{2}\mu. \tag{39}$$

The velocity can be calculated through the derivatives of the potential:

$$u_D = \frac{\mu}{4\pi}\left[\frac{z(y_1-y_2)(r_1+r_2)}{r_1r_2\{r_1r_2+[(x-x_1)(x-x_2)+(y-y_1)(y-y_2)+z^2]\}} + \right.$$

$$+\frac{z(y_2-y_3)(r_2+r_3)}{r_2r_3\{r_2r_3+[(x-x_2)(x-x_3)+(y-y_2)(y-y_3)+z^2]\}}$$

$$+\frac{z(y_3-y_4)(r_3+r_4)}{r_3r_4\{r_3r_4+[(x-x_3)(x-x_4)+(y-y_3)(y-y_4)+z^2]\}} +$$

$$\left. +\frac{z(y_4-y_1)(r_4+r_1)}{r_4r_1\{r_4r_1+[(x-x_4)(x-x_1)+(y-y_4)(y-y_1)+z^2]\}}\right], \tag{40}$$

$$v_D = -\frac{\mu}{4\pi}\left[\frac{z(x_1-x_2)(r_1+r_2)}{r_1r_2\{r_1r_2+[(x-x_1)(x-x_2)+(y-y_1)(y-y_2)+z^2]\}} + \right.$$

$$+\frac{z(x_2-x_3)(r_2+r_3)}{r_2r_3\{r_2r_3+[(x-x_2)(x-x_3)+(y-y_2)(y-y_3)+z^2]\}}$$

$$+\frac{z(x_3-x_4)(r_3+r_4)}{r_3r_4\{r_3r_4+[(x-x_3)(x-x_4)+(y-y_3)(y-y_4)+z^2]\}} +$$

$$\left. +\frac{z(x_4-x_1)(r_4+r_1)}{r_4r_1\{r_4r_1+[(x-x_4)(x-x_1)+(y-y_4)(y-y_1)+z^2]\}}\right], \tag{41}$$

$$w_D = \frac{\mu}{4\pi}\left[\frac{[(x-x_2)(y-y_1)-(x-x_1)(y-y_2)](r_1+r_2)}{r_1r_2\{r_1r_2+[(x-x_1)(x-x_2)+(y-y_1)(y-y_2)+z^2]\}} + \right.$$

$$+\frac{[(x-x_3)(y-y_2)-(x-x_2)(y-y_3)](r_2+r_3)}{r_2r_3\{r_2r_3+[(x-x_2)(x-x_3)+(y-y_2)(y-y_3)+z^2]\}}$$

$$+\frac{[(x-x_4)(y-y_3)-(x-x_3)(y-y_4)](r_3+r_4)}{r_3r_4\{r_3r_4+[(x-x_3)(x-x_4)+(y-y_3)(y-y_4)+z^2]\}} +$$

Please, cite as:
Gonzalo, J., Domínguez, D., García-Gutiérrez, A., & Escapa, A. (2020).
On the development of a parametric aerodynamic model of a stratospheric airship. Aerospace Science and Technology, 107, 106316.

$$+\frac{[(x-x_1)(y-y_4)-(x-x_4)(y-y_1)](r_4+r_1)}{r_4 r_1\{r_4 r_1+[(x-x_4)(x-x_1)+(y-y_4)(y-y_1)+z^2]\}}\Big]. \quad (42)$$

Velocities go to infinite when close to the borders of the panel, as the doublet distribution is equivalent to a ring of vortex [30].

References

1. Gonzalo J., López D., Domínguez D., García A., Escapa A., On the capabilities and limitations of high altitude pseudo-satellites. Progress in Aerospace Sciences 98, 37, 2018 (https://doi.org/10.1016/j.paerosci.2018.03.006)
2. García-Gutiérrez A., Gonzalo J., Domínguez D., López D., Escapa A., Aerodynamic optimization of propellers for High Altitude Pseudo-Satellites. Aerospace Science and Technology 96, 105562, 2020 (https://doi.org/10.1016/j.ast.2019.105562)
3. Ashraf M.Z., Choudhry M.A., Dynamic modelling of the airship with Matlab using geometrical aerodynamic parameters. Aerospace Science and Technology 25, 56, 2013 (https://doi.org/10.1016/j.ast.2011.08.014)
4. Carichner G.E., Nicolai L.M., Fundamentals of Aircraft and Airship Design, Volume 2: Airship Design and Case Studies. AIAA Education Series, 2013 (https://doi.org/10.2514/4.868986)
5. Khoury G.A. (ed.), Airship Technology, 2nd edition. Cambridge Aerospace Series 10, 2012
6. Morino L., Kuo C.C., Subsonic potential aerodynamics for complex configurations: A general theory. AIAA Journal 12, 191, 1974 (https://doi.org/10.2514/3.49191)

Please, cite as:
Gonzalo, J., Domínguez, D., García-Gutiérrez, A., & Escapa, A. (2020).
On the development of a parametric aerodynamic model of a stratospheric airship. Aerospace Science and Technology, 107, 106316.

7. Wong K.Y, Zhiyungt L., DeLaurier J., An application of source-panel and vortex methods for aerodynamic solutions of airship configurations. AIAA 85-0874, 78, 1985 (https://doi.org/10.2514/6.1985-874)

8. Erickson L.L., Panel methods—An introduction. NASA Technical Paper 2995, 1990

9. Johnson F.T, Tinoco E.N., Yu N.J., Thirty years of development and application of CFD at Boeing Commercial Airplanes, Seattle. Computers & Fluids 34, 1115, 2005 (https://doi.org/10.1016/j.compfluid.2004.06.005)

10. Wang X.L., Shan X.X., Shape optimization of stratosphere airship. Journal of Aircraft 43, 283, 2006 (https://doi.org/10.2514/1.18295)

11. Lutz T., Wagner S., Drag reduction and shape optimization of airship bodies. Journal of Aircraft 35, 345, 1998 (https://doi.org/10.2514/2.2313)

12. Li Y., Nahon M., Modeling and simulation of airship dynamics. Journal of Guidance, Control, and Dynamics 30, 1691, 2007 (https://doi.org/10.2514/1.29061)

13. Wang, X.L., Ma, Y., Shan, X.X., Modeling of stratosphere airship. Advances in Theoretical and Applied Mechanics 2, 123, 2009

14. Alam M.I., Pant R.S., Multi-objective multidisciplinary design analyses and optimization of high altitude airships. Aerospace Science and Technology 78, 248, 2018 (https://doi.org/10.1016/j.ast.2018.04.028)

15. Shen J.Q., Pan C., Wang J.J., Yi H.M., Li. T., Reynolds-number dependency of boundary-layer transition location on stratospheric airship model. Journal of Aircraft 52, 1355, 2015 (https://doi.org/10.2514/1.C032971)

Please, cite as:
Gonzalo, J., Domínguez, D., García-Gutiérrez, A., & Escapa, A. (2020).
On the development of a parametric aerodynamic model of a stratospheric airship. Aerospace Science and Technology, 107, 106316.

16. Ranneberg M., Viiflow—A New Inverse Viscous-Inviscid Interaction Method. AIAA Journal 57, 2248, 2019 (https://doi.org/10.2514/1.J058268)

17. Lutz T., Funk P., Jakobi A., Wagner S., Summary of aerodynamic studies on the LOTTE airship. In Proceedings of the 4th International Airship Convention and Exhibition, Cambridge, 2002

18. Zhang M., Wang X., Duan D., Panel method predictions of added mass for flexible airship. Aeronautical Journal 177, 519, 2013 (https://doi.org/10.1017/S0001924000008162)

19. Tuveri M., Ceruti A., Marzocca P., Added masses computation for unconventional airships and aerostats through geometric shape evaluation and meshing. International Journal of Aeronautical and Space Sciences 15, 241, 2014 (https://doi.org/10.5139/IJASS.2014.15.3.241)

20. Maskew B., Program VSAERO theory document: A computer program for calculating nonlinear aerodynamic characteristics of arbitrary configurations. NASA Contractor Report 4023, 1987

21. NEWPAN. Flow Solutions Ltd. at http://www.flowsol.co.uk/products/newpan (accessed Oct.1, 2020)

22. Johnson F.T., A general panel method for the analysis and design of arbitrary configurations in incompressible flows. NASA Contractor Report 3079, 1980

23. Ashill P.R., Wood R.F., Weeks D.J., An improved semi-inverse version of the viscous Garabedian and Korn method (VGK). *RAE* Technical Report 87002, 1987

24. Viscous full-potential (VFP) method for three-dimensional wings and wing-body combinations. Part 1: Validation of VFP results with experiment and comparisons with other methods. *ESDU 13013*, 2014

Please, cite as:
Gonzalo, J., Domínguez, D., García-Gutiérrez, A., & Escapa, A. (2020).
On the development of a parametric aerodynamic model of a stratospheric airship. Aerospace Science and Technology, 107, 106316.

25. Filkovic D., APAME – Aircraft Panel Method Tutorial: APAME version 3.0, 2010 at https://www.3dpanelmethod.com/documents/Apame%20solver%20v3.0%20Tutorial.pdf(accessed Oct. 1, 2020)

26. Fleischmann D., Weber S., Lone M.M., Fast computational aeroelastic analysis of helicopter rotor blades. *2018 AIAA Aerospace Sciences Meeting* AIAA 2018-1044, 2010 (https://doi.org/10.2514/6.2018-1044)

27. Li Y., Nahon M., Sharf I., Airship dynamics modeling: A literature review. Progress in Aerospace Sciences 47, 217, 2011 (https://doi.org/10.1016/j.paerosci.2010.10.001)

28. Funk P., Lutz T., Wagner S., Experimental investigations on hull-fin interferences of the LOTTE airship. Aerospace Science and Technology, 7, 603, 2003 (https://doi.org/10.1016/S1270-9638(03)00058-0)

29. Jones S.P., DeLaurier J.D., Aerodynamic estimation techniques for aerostats and airships. Journal of Aircraft 20, 120, 1983 (https://doi.org/10.2514/3.44840)

30. Katz J., Plotkin A., Low-Speed Aerodynamics, 2nd edition. Cambridge Aerospace Series 13, 2001

31. Ortega E., Flores R., Oñate E., A 3D low-order panel method for unsteady aerodynamic problems. International Center for Numerical Methods in Engineering, CIMNE 343, 2010

32. Ezquerro J.M., Lapuerta V., Laverón-Simavilla A., García J.M., Avilés T., Panel method for mixed configurations with finite thickness and zero thickness. Engineering Analysis with Boundary Elements 44, 28, 2014 (https://doi.org/10.1016/j.enganabound.2014.04.011)

33. Pozrikidis C., Fluid Dynamics: Theory, Computation, and Numerical Simulation, 3rd edition. Springer, 2017 (https://doi.org/10.1007/978-1-4899-7991-9)

Please, cite as:
Gonzalo, J., Domínguez, D., García-Gutiérrez, A., & Escapa, A. (2020).
On the development of a parametric aerodynamic model of a stratospheric airship. Aerospace Science and Technology, 107, 106316.

34. Band E.G.U., Payne P.R., The pressure distribution on the surface of an ellipsoid in inviscid flow. Aeronautical Quarterly 31, 70, 1980 (https://doi.org/10.1017/S0001925900008842)

35. Ramos-García N., Cayron A., Sorensen J.N., Unsteady double wake model for the simulation of stalled airfoils. Journal of Power and Energy Engineering 3, 20, 2015 (http://dx.doi.org/10.4236/jpee.2015.37004)

36. Riziotis V.A., Voutsinas S.G., Dynamic stall modelling on airfoils based on strong viscous-inviscid interaction coupling. International Journal for Numerical Methods in Fluids 56, 185, 2008 (https://doi.org/10.1002/fld.1525)

37. Prandtl L., Tietjens O.G., Applied Hydro- and Aeromechanics. Dover Publications, 1957

38. Multhopp H., Methods for calculating the lift distribution of wings: Subsonic surface lifting theory. RAE Report Aero 2353, 1950

39. Gertler M., Resistance experiments on a systematic series of streamlined bodies of revolution-for application to the design of high-speed submarines. Navy Department Report C-297, 1950

40. Hess J.L., Smith A.M.O., Calculation of potential flow about arbitrary bodies. Progress in Aerospace Sciences 8, 1, 1967 (https://doi.org/10.1016/0376-0421(67)90003-6)

Please, cite as:
Gonzalo, J., Domínguez, D., García-Gutiérrez, A., & Escapa, A. (2020).
On the development of a parametric aerodynamic model of a stratospheric airship. Aerospace Science and Technology, 107, 106316.